

## Universal rotation: how large can it be?

John D. Barrow, R. Juszkiewicz<sup>★</sup> and D. H. Sonoda

*Astronomy Centre, University of Sussex, Brighton BN1 9QH*

Accepted 1984 December 5. Received 1984 November 13

**Summary.** We present a detailed analysis of the expected temperature distribution of the cosmic microwave background radiation in flat, open and closed universes possessing small anisotropies. We predict the most general temperature patterns on the sky and their associated angular correlation functions. We use these results to evaluate the largest level of cosmic vorticity compatible with existing observations of the dipole and quadrupole fluctuations in the microwave background. This analysis extends previous work by employing the quadrupole observations and calculating all observable quantities. It is found that the asymmetries in radio-source orientations measured by Birch cannot be due to universal rotation. Detailed limits on the allowed cosmic vorticity and large-scale velocity field are given for all possible homogeneous cosmological models close to isotropy. We also study in detail the geodesic spiralling effect predicted to occur in the most general flat and open homogeneous anisotropic universes. The nature of this feature is independent of the total density in these universes and offers a new means of determining by direct observation whether or not the Universe is closed no matter how close the density is to the critical density.

### 1 Introduction

In this paper we shall derive upper limits to any large-scale rotation of the Universe by using the current observations of the dipole and quadrupole structure of the cosmic microwave background radiation. This work was provoked by a controversial paper (Birch 1982) claiming to detect a systematic trend in position angles and polarizations of high-luminosity double radio sources. It was argued that such an asymmetry can only be explained by the existence of a universal vorticity of order  $10^{-13}$  rad yr<sup>-1</sup>. Such a uniform vorticity implies that the dimensionless ratio of the vorticity,  $\omega$ , to the current Hubble expansion rate,  $H_0$ , is of order  $(\omega/H_0) \sim 10^{-3}$  but, although this is extremely large, it is not ruled out by the microwave background observations used by Collins & Hawking in their 1973 study of the rotation and distortion of the Universe (Collins & Hawking 1973).

<sup>★</sup> Copernicus Astronomical Centre, Bartycka 18, 00715 Warsaw, Poland.

It is not our intention to enter here into a discussion of Birch's observations or their statistical significance (Phinney & Webster 1983; Birch 1983; Kendall & Young 1984; Kendall 1984). We shall show that a universal vorticity at the level claimed by Birch is incompatible with existing observations of the microwave background and we shall also produce detailed temperature maps for models containing rotation and show that a detection of large-scale rotation in the Universe has a number of important consequences for determinations of the total density of the Universe and elementary particle physics.

Our analysis of the evolution and structure of vorticity in the Universe will assume, to a first approximation, that this vorticity is spatially homogeneous. This will allow us to model it using linearizations of homogeneous, anisotropic cosmological models about the isotropic Friedmann universes. This is the approach used first by Hawking (1969) and then by Collins & Hawking (1973) in their earlier studies. Our analysis improves and extends these papers in a variety of ways. We employ the most recent observations of the quadrupole variation of the microwave temperature anisotropy and not simply the weaker, dipole fluctuation limits (Fixsen, Cheng & Wilkinson 1983; Lubin, Epstein & Smoot 1983). Besides improving the upper limits sufficiently to rule out Birch's claim this refinement also allows us to use linearized theory self-consistently [this was not possible in earlier studies (Collins & Hawking 1973) as their authors' point out: microwave background fluctuations could be large enough to allow the shear anisotropy to have been of order unity at redshifts less than that of last scattering,  $z_E \lesssim 10^3$ ]. Whereas Collins & Hawking concentrated upon deriving approximate analytic limits on the magnitude of the vorticity, we have performed detailed numerical computations of the limits and have also determined the angular temperature profiles,  $T(\theta, \phi)$ , over the sky. In order to relate our predictions more closely to the quantities actually measured we have also indicated the smoothing effects introduced over small angular scales by finite beamwidths and cosmological reheating.

It is clearly of considerable cosmological importance to determine whether or not universal rotation exists at a measurable level. Besides shedding further light on the physical significance of Mach's Principle (Raine 1975; Raine & Heller 1981), it has consequences for our understanding of high-energy physics and processes occurring in the neighbourhood of the initial singularity. If the 'inflationary' picture (Gibbons, Hawking & Siklos 1983; Barrow & Turner 1982) of the very early Universe is correct then quantum fluctuations of a self-interacting scalar field can be inflated to create a spectrum of scalar density (Hawking 1982a; Starobinskii 1982) or tensor gravitational wave fluctuations with virtually (Abbott & Wise 1984; Starobinskii 1979) a constant curvature form. However, the *scalar* nature of the Higgs field that leads to those large-scale perturbations ensures that any velocity perturbations generated by the inflation process must be curl-free and any vorticity existing prior to the process of inflation should be exponentially damped (Barrow 1977, 1983; Ellis & Olive 1983) if it has not already been dissipated by particle creation effects (Lukash, Novikov & Starobinskii 1976) or excluded *ab initio* by boundary conditions required for the consistency of quantum theory and general relativity (Barrow 1978; Penrose 1979; Hawking 1982b; Barrow & Tipler 1985). The absence of universal rotation is a prediction of the inflationary universe picture.

In order to study the evolution of vorticity in universes that resemble our own we shall investigate the behaviour of the most general anisotropic, spatially homogeneous generalizations of the Friedmann universes in the approximation of small anisotropies. We shall calculate the microwave background temperature profiles and multipole moments as functions of the induced shear and determine the maximum vorticity allowed in open, closed and flat Friedmann background universes by confronting these predicted temperature profiles with observation. In Sections 2 and 3 we introduce, with a minimum of detail,

the basic equations and quantities necessary to present our results. In Section 4 we present and discuss the results for the cases of open and flat universes, while in Section 5 we do the same for the case of a closed universe. Then, in Section 6 we discuss the effects of cosmological reheating and finite antenna beamwidth upon our results before summarizing our conclusions in Section 7.

## 2 Basic equations

We shall employ the formalism introduced by Collins & Hawking to consider the most general spatially homogeneous perturbations of the Friedmann models. For the flat, open and closed Friedmann universes these perturbations are presented by linearizations about the Friedmann models of the Bianchi VII<sub>0</sub>, VII<sub>h</sub> and IX models respectively. We shall compute the angular variation of the microwave background temperature,  $T(\theta, \phi)$ , over the sky relative to the mean temperature  $T_0$ , and put

$$\frac{\Delta T}{T} \equiv \frac{T(\theta, \phi) - T_0}{T_0}. \quad (2.1)$$

The associated angular correlation function  $W(\theta)$  is defined by

$$W(\theta) = \langle \Delta T(\gamma) \Delta T(\gamma') \rangle T_0^{-2}. \quad (2.2)$$

where  $\gamma$  and  $\gamma'$  are unit vectors and  $\gamma \cdot \gamma' = \cos \theta$ . The average  $\langle \dots \rangle$  is over all pairs of points on the celestial sphere having angular separation  $\theta$ .

Observational constraints on the allowed deviations from isotropy caused by cosmic vorticity will be imposed by comparing the predicted and observed dipole and quadrupole fluctuations in  $T(\theta, \phi)$ . The required decomposition of  $T(\theta, \phi)$  into spherical harmonics is

$$\frac{\Delta T}{T} = \sum_{l=1}^{\infty} \sum_{m=-l}^l a_{lm} Y_{lm}(\theta, \phi), \quad (2.3)$$

where

$$Y_{lm}(\theta, \phi) = \left[ \frac{(2l+1)(l-|m|)!^{1/2}}{4\pi(l+|m|)!} \right] P_l^{|m|}(\cos \theta) \exp(im\phi) \cdot \begin{cases} (-1)^m & m \geq 0 \\ 1 & m < 0 \end{cases}, \quad (2.4)$$

with

$$a_{lm} = \int_0^{2\pi} d\phi \int_0^\pi \left( \frac{\Delta T}{T} \right) Y_{lm}^* \sin \theta d\theta, \quad (2.5)$$

where  $P_l^m$  are Associated Legendre Polynomials and \* denotes complex conjugation.

The spatially homogeneous models admit a 3-parameter group of symmetries on a family of space-like hypersurfaces (MacCallum 1979). These surfaces can be labelled by a time parameter  $t$  such that  $g^{\alpha\beta} n_\alpha n_\beta = -1$ , where  $n_\alpha = -t_{;\alpha}$  is the normal to the hypersurface (; denotes covariant differentiation and Greek indices run 0 to 3). The metric can be written

$$g_{\mu\nu} = -n_\mu n_\nu + g_{AB} E_\mu^A E_\nu^B, \quad (2.6)$$

where  $g_{AB}$  is a  $3 \times 3$  matrix depending only on  $t$ . The  $E_\mu^A$  are three invariant covector fields on the surfaces of homogeneity chosen to obey the relations

$$E_{\mu;\nu}^A - E_{\nu;\mu}^A = C_{BC}^A E_\mu^B E_\nu^C, \quad (2.7)$$

where the  $C_{BC}^A$  are the canonical structure constants for the symmetry group (upper case latin indices run 1 to 3). Following Misner (1968), we can decompose the metric as

$$g_{AB} = \exp(2\alpha) [\exp(2\beta)]_{AB} \quad (2.8)$$

where the scalar  $\alpha$  represents the volumetric expansion whilst the trace-free symmetric matrix  $[\exp(2\beta)]_{AB}$  includes the anisotropy. In the orthonormal basis of Collins & Hawking the shear tensor is given by the matrix equation, ( $\dot{\phantom{x}} = d/dt$ ),

$$\sigma_{ij} = 1/2 [(e^\beta)^\cdot (e^{-\beta}) + (e^{-\beta})(e^\beta)^\cdot]_{ij}. \quad (2.9)$$

In this basis  $i, j$  run 1 to 3 and are unchanged under raising and lowering operations whereas the 0 component changes sign. For small anisotropies

$$\sigma_{ij} \approx \dot{\beta}_{ij}. \quad (2.10)$$

We shall consider the Universe to be dominated by pressureless matter after recombination. The stress tensor is therefore

$$T_{ab} = \rho u_a u_b, \quad (2.11)$$

where  $\rho$  is the energy density and  $u_a$  the fluid four-velocity vector. Since our models will possess small anisotropies we require

$$\beta_{ij} \ll 1, \quad |u_i| \ll 1, \quad |\sigma_{ij}| \ll \dot{\alpha}. \quad (2.12)$$

We shall be especially interested in the vorticity

$$\omega \equiv (g_{AB} \omega^A \omega^B)^{1/2} = (\omega^i \omega_i)^{1/2}. \quad (2.13)$$

In the  $E_A^\mu$  basis we have

$$\omega^A = 1/2 \exp(-3\alpha) \epsilon_{ABC} [1/2 C_{BC}^D u_D u^0 + u_B \dot{u}_C] \quad (2.14)$$

from the conservation equations  $T_{;\nu}^{\mu\nu} = 0$ , where  $\epsilon_{ABC}$  is the completely antisymmetric tensor of rank 3. For small (non-relativistic) velocities  $u^0 \sim 1$  and  $u_A$  is small, so

$$\omega^A \approx 1/4 \exp(-3\alpha) \epsilon_{ABC} C_{BC}^D \mu_D. \quad (2.15)$$

The angular dependence of the cosmological redshift is given by

$$1 + z_E = \frac{(K^\mu u_\mu)_E}{(K^\mu u_\mu)_0} \quad (2.16)$$

where  $K^\mu$  is the tangent vector to the null geodesic from the observer in a given direction. The subscripts E and 0 refer to the photon emission and reception events respectively. This expression can be related to the temperature anisotropy since

$$T_0 = \frac{T_E}{1 + z_E(\theta_0, \phi_0)}. \quad (2.17)$$

To first order, (2.16) and (2.17) give

$$\frac{\Delta T(\theta_0, \phi_0)}{T_0} = (p^i u_i)_0 - (p^i u_i)_E - \int_E^0 p^j p^k \sigma_{jk} dt. \quad (2.18)$$

The  $p^i = (\cos \theta, \sin \theta \cos \phi, \sin \theta \sin \phi)$  are the direction cosines of the null geodesics towards the observer in the unperturbed Friedmann model. Since  $\theta_0$  and  $\phi_0$  specify the direction of the incoming photon they are not the observing angles on the sky ( $\theta_{\text{ob}}, \phi_{\text{ob}}$ ), but they are related to them by

$$\theta_{\text{ob}} = \pi - \theta_0, \quad \phi_{\text{ob}} = \pi + \phi_0. \quad (2.19)$$

For convenience we shall perform calculations using  $\theta_0$  and  $\phi_0$  and only convert to  $\theta_{\text{ob}}$  and  $\phi_{\text{ob}}$  when we display the temperature patterns expected on the celestial sphere.

The first term on the right of (2.18) gives a dipole temperature variation due to our motion relative to the hypersurfaces of constant time in the Universe when the photons are received. The second term on the right of (2.18) is an analogous ‘Doppler’ variation due to the peculiar motion of the source at the last scattering redshift which we take to be  $1 + z_E = 10^3$ ; it will not, in general, contribute a pure dipole temperature variation. These two contributions will be absent in models where the matter flow is orthogonal to the hypersurfaces of homogeneity, in which case the velocities  $u^i$  are comoving, but they will be present in ‘tilted’ models (Ellis & King 1974) with non-comoving velocities. The final integral term in (2.18) gives the distortion anisotropy in the temperature profile introduced by the anisotropic expansion. Only in special models is this purely a quadrupole variation.

The time-dependence of  $u_i$  and  $\sigma_{ij}$  are obtained from the Einstein equations whilst the geodesic equations (see Appendix A) give the variation of  $\theta$  and  $\phi$  with time. If we then express everything in terms of  $\theta_0$  and  $\phi_0$  we obtain the pattern that would now be seen after using (2.19) to convert to the observing angles  $\theta_{\text{ob}}$  and  $\phi_{\text{ob}}$ .

In fact, before displaying predictions of  $T(\theta_{\text{ob}}, \phi_{\text{ob}})$  and  $W(\theta_{\text{ob}})$  we should account for the smoothing effects of finite antenna beamwidth and reheating of the cosmic medium. If  $\overline{\Delta T}(\theta, \phi)/T_0$  and  $\overline{W}(\theta)$  describe the temperature anisotropy after Gaussian smoothing, we calculate them from  $\Delta T(\theta, \phi)/T_0$  and  $W(\theta)$  using

$$\frac{\overline{\Delta T}(\theta, \phi)}{T_0} = \iint \sin \theta' \frac{\Delta T(\theta', \phi')}{T_0} f(|\boldsymbol{\gamma} - \boldsymbol{\gamma}'|, y) d\theta' d\phi', \quad (2.20)$$

$$\begin{aligned} \overline{W}(\theta) &= \frac{1}{2y^2} \int W(\alpha) \alpha \exp\left[-\frac{(\alpha^2 + \theta^2)}{4y^2}\right] I_0\left(\frac{\alpha\theta}{2y^2}\right) d\alpha \\ &\equiv \frac{\langle \overline{\Delta T}(\boldsymbol{\gamma}) \overline{\Delta T}(\boldsymbol{\gamma}') \rangle}{T_0^2} \end{aligned} \quad (2.21)$$

where  $f(|\boldsymbol{\gamma} - \boldsymbol{\gamma}'|, y)$  is the two-dimensional Gaussian

$$f(x, y) = (2\pi y^2)^{-1} \exp\left[-\frac{x^2}{2y^2}\right] \quad (2.22)$$

and  $I_0(x)$  is the modified Bessel function with  $\boldsymbol{\gamma}' \equiv (\sin \theta' \cos \phi', \sin \theta' \sin \phi', \cos \theta')$  and  $\boldsymbol{\gamma} \cdot \boldsymbol{\gamma}' = \cos \theta$ . Fixsen *et al.* (1983) use an antenna with a beamwidth of  $\Delta_A = 7^\circ$ . If  $\Delta_R = 5^\circ \Omega_0^{1/3}$  is the angular scale of smoothing due to secondary ionization of the intergalactic medium, then we can simply interpret  $\Delta$  in (2.20)–(2.22) as an effective  $\Delta = (\Delta_R^2 + \Delta_A^2)^{1/2}$  in order to include the effects of reheating and beam smoothing; this will be discussed in Section 6.

### 3 Quasi-Friedmann universes

We shall be interested in the most general spatially homogeneous universes that contain the Friedmann models as special cases. These are the Bianchi types VII<sub>h</sub> and IX which contain

the open and closed Friedmann models respectively. The less general type  $VII_0$  model contains the flat Friedmann model as a sub-case. The extensively studied cosmological models of Bianchi types I and V are just special subcases of the  $VII_0$  and  $VII_h$  models. The type I geometry is so special that no vortical motions of perfect fluid are allowed,  $T_{\alpha 0} \equiv 0$ . We shall consider microwave background profiles in type  $VII_h$  and IX models, and by suitable specialization of parameters the results for types I, V and  $VII_0$  perturbations of Friedmann models can be read-off as required. To give this specialization procedure we note that Bianchi types  $VII_0$  and  $VII_h$  contain a free parameter,  $x$ , identified by Collins & Hawking. It is related to  $h$  in the  $VII_h$  model via

$$x = \left( \frac{h}{1 - \Omega_0} \right)^{1/2}. \quad (3.1)$$

Its physical meaning is related to the characteristic wavelength over which the principal axes of shear and rotation change orientation,

$$x = \frac{\text{comoving scale on which basis vectors change orientation}}{\text{horizon size}}. \quad (3.2)$$

To be in accord with observations of the Universe's large-scale uniformity, and to justify a homogeneous model as a description, one should restrict interest to models with  $x \geq 0.04$  where the lower bound is given by the scale of observed superclustering. We shall, however, examine the influence of a wide range of values of  $x$  on the  $\Delta T/T_0$  predictions.

A type  $VII_h$  solution is partially described by the parameters  $\Omega_0 < 1$  and  $x$  (or  $h$ ). By taking various limits of these parameters the I, V and  $VII_0$  solutions can be obtained, as shown in Fig. 1a.

In previous investigations (Barrow, Juszkiewicz & Sonoda 1983) of the possible microwave background patterns arising in anisotropic models we showed there exists a division between those producing pure quadrupole variations and those open ( $\Omega_0 < 1$ ) models which exhibit a focusing of the quadrupole pattern into a 'hotspot'. We shall see that the  $VII_0$  and  $VII_h$  models introduce another effect which is superimposed upon the basic quadrupole or

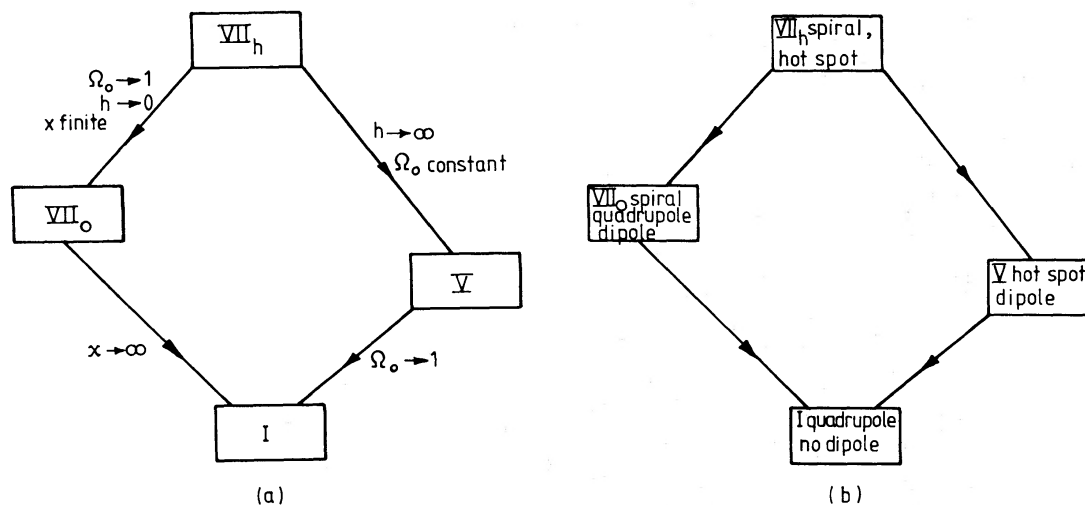


**Figure 1.** (a) The relationship of the Bianchi I, V,  $VII_0$  and  $VII_h$  cosmological models employed in the text (Sections 4 and 5). The  $VII_h$  models are parametrized by  $\Omega_0$  and  $x$ , which are related to  $h$  by equation (3.1). The types V,  $VII_0$  and I are derived from  $VII_h$  by taking the limits indicated in the figure. (b) The qualitative form of the microwave temperature pattern,  $\Delta T(\theta, \phi)/T_0$ , arising in the Bianchi types I, V,  $VII_0$  and  $VII_h$  close to isotropy. Positions of models are as in Fig. 1(a). The open ( $\Omega_0 < 1$ ) universes exhibit 'hotspots' and the type VII universes 'spirals'.

hotspot pattern: a spiralling effect introduced by the intrinsic handedness of their three-geometrics. This spiral effect was noticed first by Collins & Hawking and later by Doroshkevich, Lukash & Novikov (1975) but temperature maps including this feature have not been produced before. The possible combinations of microwave features are exhibited schematically in Fig. 1b.

The Bianchi type IX model is distinct from those of type VII<sub>h</sub> and so closed universes will be discussed separately in Section 5. We shall see that investigations of vorticity may offer a means of distinguishing between open and closed universes no matter how close  $\Omega_0$  lies to unity.

#### 4 Open and flat universes

In this section we shall give explicit results for the VII<sub>h</sub> universes linearized about the open Friedmann model. The unperturbed Friedmann model is described by an expansion scale factor

$$e^\alpha = \frac{h^{1/2} \Omega_0}{H_0(1 - \Omega_0)^{3/2}} \operatorname{sh}^2\left(\frac{h^{1/2} \tau}{2}\right) \equiv \frac{dt}{d\tau}. \quad (4.1)$$

The present value of the scale factor can be arbitrarily chosen, but

$$e^{\alpha_0} = \frac{h^{1/2}}{H_0(1 - \Omega_0)^{1/2}} = \frac{x}{H_0}. \quad (4.2)$$

So, the parameter  $x$  has no physical meaning in the Friedmann models. It can be scaled out of the solution but it is included to establish continuity with the VII<sub>h</sub> models where the shear is non-zero and it does have an invariant physical interpretation (3.2) (see Collins & Hawking 1973).

We shall calculate the contribution to  $\Delta T/T_0$  from the vorticity alone. The inclusion of other pure shear distortions which are independent of the rotation could only make  $\Delta T/T_0$  larger. Hence, our results will give the maximum level of vorticity consistent with a given value of  $\Delta T/T_0$ .

In VII<sub>h</sub> cosmological models we have two independent vorticity components,  $\omega^2$  and  $\omega^3$ , and they can be described in terms of the off-diagonal shear modes,  $\sigma_{12}$  and  $\sigma_{13}$ , which they induce,

$$\omega_2 = \frac{(3h - 1)\sigma_{13} - 4h^{1/2}\sigma_{12}}{3x^2\Omega_0}, \quad (4.3)$$

$$\omega_3 = \frac{(1 - 3h)\sigma_{12} - 4h^{1/2}\sigma_{13}}{3x^2\Omega_0}. \quad (4.4)$$

There are two dimensionless amplitudes to be constrained by observation:  $(\sigma_{12}/H)_0$  and  $(\sigma_{13}/H)_0$ . They are related to the present dimensionless measure of vorticity scalar to Hubble rate,  $(\omega/H)_0$ , by the velocity components  $u_2$  and  $u_3$  via

$$\omega = \frac{1}{2} e^{-\alpha} (1 + h)^{1/2} [(u_2)^2 + (u_3)^2]^{1/2}, \quad (4.5)$$

where

$$(u_2)_0 = \frac{1}{3x\Omega_0} \left[ 3h^{1/2} \left(\frac{\sigma_{12}}{H}\right)_0 - \left(\frac{\sigma_{13}}{H}\right)_0 \right], \quad (4.6)$$

$$(u_3)_0 = \frac{1}{3x\Omega_0} \left[ \left(\frac{\sigma_{12}}{H}\right)_0 + 3h^{1/2} \left(\frac{\sigma_{13}}{H}\right)_0 \right], \quad (4.7)$$

and hence the present vorticity is given by

$$\left(\frac{\omega}{H}\right)_0 = \frac{(1+h)^{1/2}(1+9h)^{1/2}}{6x^2\Omega_0} \left[ \left(\frac{\sigma_{12}}{H}\right)_0^2 + \left(\frac{\sigma_{13}}{H}\right)_0^2 \right]^{1/2}. \quad (4.8)$$

Using the solution of the geodesic equations given in the Appendix we find the expected temperature anisotropy in terms of  $\Omega_0$ ,  $h$   $(\sigma_{12}/H)_0$  and  $(\sigma_{13}/H)_0$  as

$$\begin{aligned} \frac{\Delta T}{T_0} = & \frac{(1-\Omega_0)^{1/2}}{3\Omega_0 h^{1/2}} \left\{ \left[ 3h^{1/2} \left(\frac{\sigma_{12}}{H}\right)_0 - \left(\frac{\sigma_{13}}{H}\right)_0 \right] [\sin \theta_0 \cos \phi_0 - \sin \theta_E \cos \phi_E (1+z_E)] \right. \\ & \left. + \left[ \left(\frac{\sigma_{12}}{H}\right)_0 + 3h^{1/2} \left(\frac{\sigma_{13}}{H}\right)_0 \right] [\sin \theta_0 \sin \phi_0 - \sin \theta_E \sin \phi_E (1+z_E)] \right\} \\ & - \int_{\tau_E}^{\tau_0} \frac{h^{1/2}(1-\Omega_0)^{3/2}}{\Omega_0^2} \sin 2\theta \left[ \left(\frac{\sigma_{12}}{H}\right)_0 \cos \phi + \left(\frac{\sigma_{13}}{H}\right)_0 \sin \phi \right] \frac{d\tau}{\text{sh}^4(h^{1/2}\tau/2)} \end{aligned} \quad (4.9)$$

where

$$\begin{aligned} \tau_0 &= 2h^{-1/2} \text{sh}^{-1} [(\Omega_0^{-1} - 1)^{1/2}], \\ \tau_E &= 2h^{-1/2} \text{sh}^{-1} \left[ \frac{(\Omega_0^{-1} - 1)^{1/2}}{1+z_E} \right]. \end{aligned} \quad (4.10)$$

The qualitative behaviour of the geodesics can be seen from equations (A. 10). There is a focusing effect due to the variation of  $\theta$  with  $\tau$  which is similar to that calculated for type V in the absence of rotation. In addition, there is a spiralling of the geodesics created by the variation of  $\phi$  with  $\tau$ . The formulae given above give the correct results for VII<sub>0</sub> in the limit  $h \rightarrow 0$ ,  $\Omega_0 \rightarrow 1$  with  $x$  finite, and for type V as  $h \rightarrow \infty$  (see Fig. 1a) and include various minor numerical and algebraic corrections to the earlier calculations in ref. (2).

It is convenient to decompose (4.9) into the form

$$\begin{aligned} \frac{\Delta T}{T_0}(\theta_0, \phi_0) = & \left[ \left(\frac{\sigma_{12}}{H}\right)_0 A(\theta_0) + \left(\frac{\sigma_{13}}{H}\right)_0 B(\theta_0) \right] \sin \phi_0 \\ & + \left[ \left(\frac{\sigma_{12}}{H}\right)_0 B(\theta_0) - \left(\frac{\sigma_{13}}{H}\right)_0 A(\theta_0) \right] \cos \phi_0, \end{aligned} \quad (4.11)$$

where we have defined  $A(\theta_0)$  and  $B(\theta_0)$  by

$$\begin{aligned} A(\theta_0) \equiv & C_1 [\sin \theta_0 - C_2 (\cos \psi_E - 3h^{1/2} \sin \psi_E)] \\ & + C_3 \int_{\tau_E}^{\tau_0} \frac{s(1-s^2) \sin \psi d\tau}{(1+s^2)^2 \text{sh}^4(h^{1/2}\tau/2)}, \end{aligned} \quad (4.12)$$

$$\begin{aligned} B(\theta_0) \equiv & C_1 [3h^{1/2} \sin \theta_0 - C_2 (\sin \psi_E + 3h^{1/2} \cos \psi_E)] \\ & - C_3 \int_{\tau_E}^{\tau_0} \frac{s(1-s^2) \cos \psi d\tau}{(1+s^2)^2 \text{sh}^4(h^{1/2}\tau/2)}, \end{aligned} \quad (4.13)$$

with  $C_1$ ,  $C_2$ ,  $C_3$ ,  $s$ , and  $\psi$  defined by

$$C_1 \equiv (3\Omega_0 x)^{-1}; \quad C_2 \equiv \frac{2s_E(1+z_E)}{1+s_E^2}; \quad C_3 \equiv 4h^{1/2}(1-\Omega_0)^{3/2}\Omega_0^{-2}; \quad (4.14)$$

$$s \equiv \tan\left(\frac{\theta}{2}\right) = \tan\left(\frac{\theta_0}{2}\right) \exp[-h^{1/2}(\tau - \tau_0)], \quad (4.15)$$

$$\psi = (\tau - \tau_0) - h^{-1/2} \ln \left\{ \sin^2\left(\frac{\theta_0}{2}\right) + \exp[2h^{1/2}(\tau - \tau_0)] \cos^2\left(\frac{\theta_0}{2}\right) \right\}. \quad (4.16)$$

Thus, numerical computations of  $\Delta T(\theta, \phi)/T_0$  due to rotation in all the Bianchi types V, VII<sub>o</sub> and VII<sub>h</sub> just involve computations of  $A(\theta_0)$  and  $B(\theta_0)$  for the appropriate choice of  $z_E$ ,  $\Omega_0$  and  $x$  [or  $h$ , if we recall equation (3.1)]. The required system of equations linking the vorticity,  $(\omega/H)_0$  to the temperature profile is given by (4.8) and (4.10–4.16).

Since we shall be confronting the theoretical predictions with observations of the dipole and quadrupole moments of  $\Delta T/T_0$ , it is expedient to express all temperature anisotropy moments in terms of the vorticity. Using (4.11) and (2.3)–(2.5) we can calculate the multipole moments  $a_{lm}$ , which we write as  $a_{l\pm}$  since only the sign of  $m$  matters in (2.4),

$$a_{l\pm} = \mp i\pi \left[ \left(\frac{\sigma_{12}}{H}\right)_0 I_{lA} + \left(\frac{\sigma_{13}}{H}\right)_0 I_{lB} \right] \\ \mp \left[ \left(\frac{\sigma_{12}}{H}\right)_0 I_{lB} - \left(\frac{\sigma_{13}}{H}\right)_0 I_{lA} \right], \quad (4.17)$$

where we have defined

$$I_{lA} \equiv \left[ \frac{2l+1}{4\pi l(l+1)} \right]^{1/2} \int_0^\pi A(\theta) P_l^1(\cos\theta) \sin\theta \, d\theta \quad (4.18)$$

$$I_{lB} = \left[ \frac{2l+1}{4\pi l(l+1)} \right]^{1/2} \int_0^\pi B(\theta) P_l^1(\cos\theta) \sin\theta \, d\theta. \quad (4.19)$$

Therefore, if we define

$$a_l^2 \equiv \frac{1}{4\pi} \sum_{m=-l}^l |a_{lm}|^2 \quad (4.20)$$

we have

$$a_l = \left(\frac{\pi}{2}\right)^{1/2} (I_{lA}^2 + I_{lB}^2)^{1/2} \left[ \left(\frac{\sigma_{12}}{H}\right)_0^2 + \left(\frac{\sigma_{13}}{H}\right)_0^2 \right]^{1/2}. \quad (4.21)$$

Observational limits on the dipole and quadrupole moments of the background radiation anisotropy,  $a_1$  and  $a_2$ , will therefore give us upper limits on  $[(\sigma_{12}/H)_0^2 + (\sigma_{13}/H)_0^2]^{1/2}$  and hence on the vorticity  $(\omega/H)_0$  by using (4.8). We note that using  $\theta_0$  and  $\phi_0$  instead of the observing angles  $\theta_{ob}$  and  $\phi_{ob}$ , (see 2.19) only introduces a factor of  $(-1)^l$  into the formula (2.5) for  $a_{lm}$ .

In Figs 2 and 3 we show plots of  $T(\theta, \phi)$  for the VII<sub>o</sub> and VII<sub>h</sub> models with  $x = 0.067$  (this is the smallest value of  $x$  that is realistic). The qualitative features shown there are not peculiar to the presence of rotation but would appear in VII<sub>o</sub> and VII<sub>h</sub> models containing pure shear anisotropy with zero vorticity also.

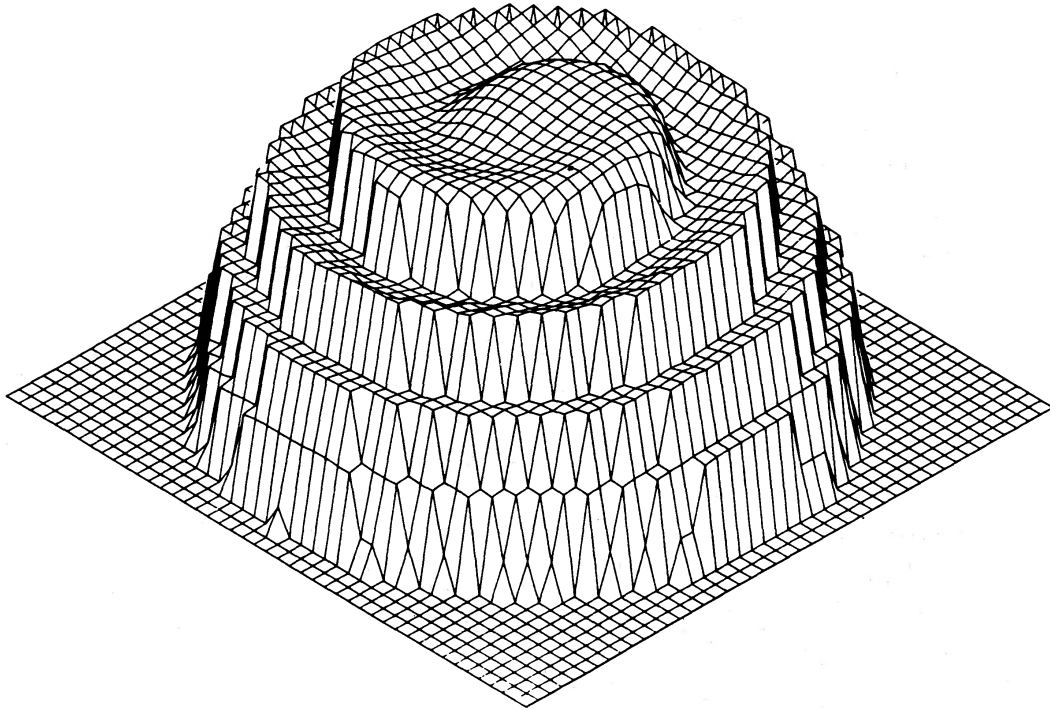


**Figure 2.** The temperature pattern,  $T(\theta, \phi)$ , predicted in a type  $VII_0$  universe ( $\Omega_0 = 1$ ) in the region  $0 < \phi_{0b} < 2\pi$ ,  $\pi/2 \leq \theta_{0b} < \pi$ . The radial distance represents the magnitude of  $T(\theta_{0b}, \phi_{0b})$ . The profile is for a model with the maximum vorticity compatible with observation when  $x = 0.067$  (see Table 3). The redshift of last scattering is  $1 + z_E = 10^3$ . For simplicity we have chosen  $(\sigma_{12}/H)_0 = (\sigma_{13}/H)_0$  but choosing differently just rotates the whole pattern in the angle  $\phi_0 \rightarrow \phi_0 + \text{constant}$ . The left-handed geodesic spiralling effect discussed in the text is clearly evident.

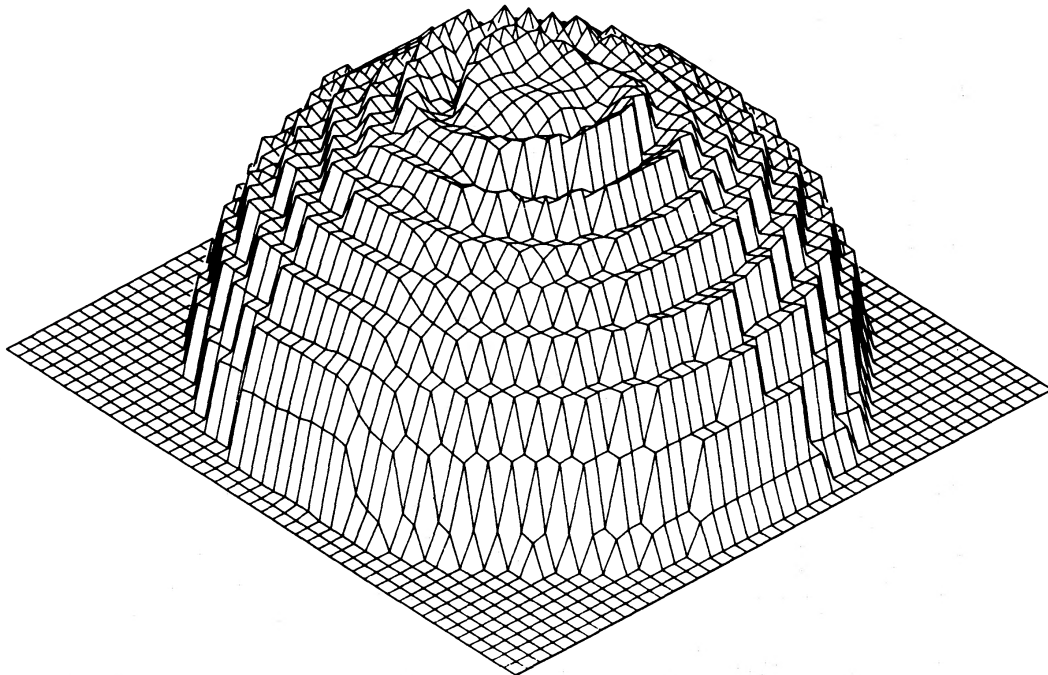


**Figure 3.** As Fig. 2 but for an open  $VII_h$  Universe with  $\Omega_0 = 0.7$  and  $x = 0.067$ . The negative curvature is responsible for a ‘hotspot’ effect which focuses the left-handed spiral temperature pattern towards the axis  $\theta_{0b} = \pi$ . The total number of spiral twists is determined by  $x$ , equation (4.25), and is unaffected by  $\Omega_0$ .

Fig. 2 is the pattern created in a flat ( $\Omega_0=1$ ) universe containing small-amplitude vorticity or shear. The underlying quadrupole plus dipole pattern is modulated by the spiralling effect of the geodesics in the  $\phi$  plane; as  $x \rightarrow \infty$  the spiral spacing increases and the entire pattern approaches the pure quadrupole expected in Bianchi type I. In Fig. 3, we see the same spiral phenomenon is displayed by the open ( $\Omega_0 < 1$ ) universe of Bianchi type VII<sub>h</sub> when close to isotropy. In this case the geodesic focusing in the  $\theta$  coordinate, discussed in detail by Barrow *et al.* (1983), squeezes the spiral quadrupole and dipole seen in Fig. 2 into a region of smaller angular scale. As  $x \rightarrow \infty$  the spiral spacing grows and the pattern becomes identical to that found in Bianchi type V models containing vortical modes. From these figures one can see how a very small value of  $x$  would create extremely irregular temperature profiles over small angular scales. Notice that the spirals have a definite handedness; this arises because of the intrinsic group of motions underlying the Bianchi type VII<sub>h</sub> geometry. A similar effect was noted in connection with the polarization of the microwave background by Matzner & Tolman (1982).

At this juncture it is worth discussing the 'spiral' geodesic effect in more detail. In the models we have been describing in this section the temperature patterns can all be expressed in the form (4.11) with  $A(\theta_0)$  and  $B(\theta_0)$  differing from model to model as prescribed by (4.12–4.16). We can rearrange (4.11) as

$$\frac{\Delta T}{T_0} = (A^2 + B^2)^{1/2} \left( \frac{\sigma}{H} \right)_0 \cos(\phi_0 + \tilde{\phi}) \quad (4.22)$$

where  $\tilde{\phi}$  is given by

$$\cos \tilde{\phi} = \left[ \left( \frac{\sigma_{12}}{\sigma} \right)_0 B - \left( \frac{\sigma_{13}}{\sigma} \right)_0 A \right] (A^2 + B^2)^{-1/2}. \quad (4.23)$$

So, if we look around any circle of given  $\theta_0$  on the sky, the temperature variation will possess a pure  $\cos \phi_0$  dependence. The type V, VII<sub>o</sub> and VII<sub>h</sub> temperature patterns differ only in the amplitude of this  $\cos \phi_0$  variation and in the relative orientation of adjacent  $\theta_0 = \text{constant}$  rings, which are labelled by  $\tilde{\phi}$ . For type V we have  $A(\theta_0) = 0$  so  $\tilde{\phi}$  is constant and there is no spiralling; the amplitude of  $\Delta T/T_0$  and the focusing into a hotspot are determined by  $B(\theta_0)$ .<sup>\*</sup> For type VII<sub>o</sub> and VII<sub>h</sub> universes the parameters  $A(\theta_0)$  and  $B(\theta_0)$  are both non-zero and this leads to the twisting of the overall profile. For a large redshift of last scattering,  $A$  and  $B$  are approximately of the form

$$\{A(\theta), B(\theta)\} \sim \left. \begin{array}{l} \sin [(2 \cos \theta_0)/x] \\ \text{or} \\ \cos [(2 \cos \theta_0)/x] \end{array} \right\} f(x, \theta_0) \quad (4.24)$$

for some function  $f(x, \theta_0)$ . Hence, we see there will be roughly  $N$  complete twists of the full spiral pattern with

$$N \sim \frac{2}{\pi x} \quad (4.25)$$

since there is a complete spiral twist whenever  $2 \cos \theta_0 = 2 m \pi x$ ,  $m$  integral. The smaller  $x$ , so the smaller the scale over which the shear and vorticity basis vectors change their orientation (see equation 3.2), and the tighter the resulting spiral. These cosmological models have a

<sup>\*</sup> In the limit  $\Omega_0 \rightarrow 1$ ,  $B(\theta_0) \sim [(1 + z_E)^{3/2} - 1] \sin 2\theta_0$  and the type V pattern reduces to the pure quadrupole of type I.

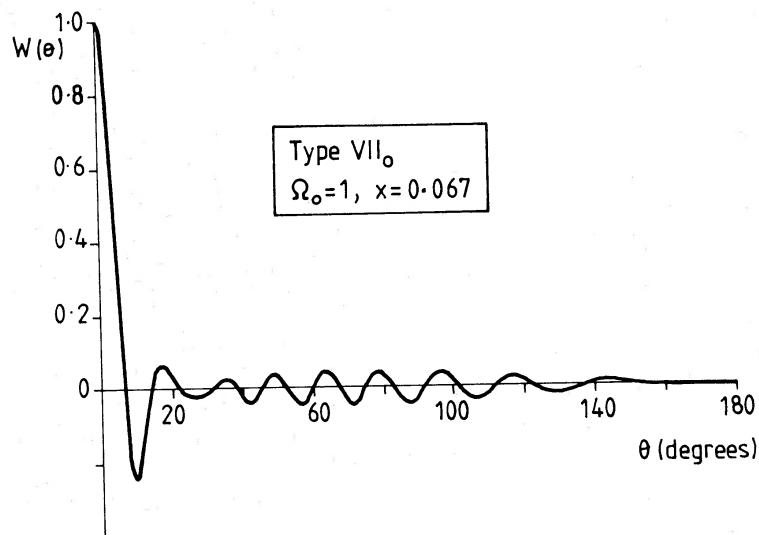


**Figure 4.** The unsmoothed correlation function,  $W(\theta)$ , defined by equation (2.2) for a type VII<sub>0</sub> universe with  $\Omega_0 = 1$  and  $x = 0.067$ .  $W(\theta)$  has been scaled so  $W(0) = 1$  and, in line with observers' practice, the dipole component of  $\Delta T/T_0$  was subtracted before calculating  $W(\theta)$ . The observations of Fixsen *et al.* (1983), and Lubin *et al.* (1983) give limits of  $W(\theta) < 9 \times 10^{-10}$  for  $\theta > 10^\circ$  which limits the allowed vorticity in this model today to  $(\omega/H)_0 < 10^{-7}$  and the associated peculiar velocities to  $(u)_0 < 2 \times 10^{-8}$  (in units of  $c$ ).

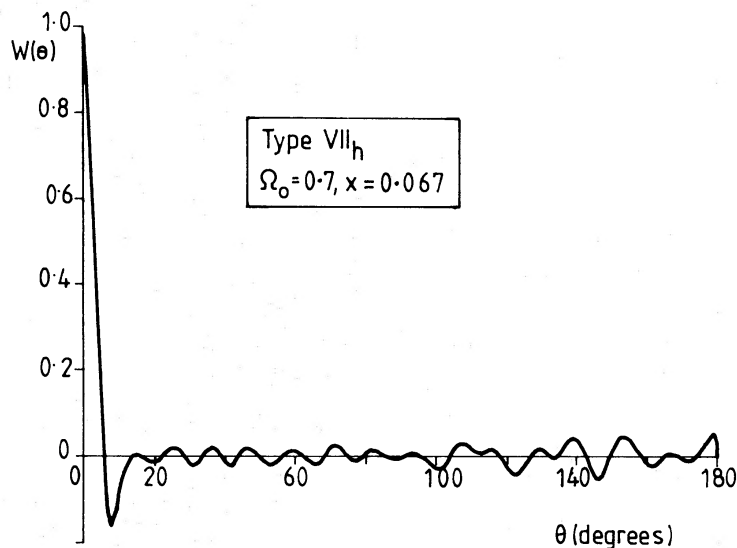


**Figure 5.** The unsmoothed correlation function,  $W(\theta)$ , as Fig. 4, for a type VII<sub>h</sub> universe with  $\Omega_0 = 0.7$  and  $x = 0.067$ . The observational bounds on  $W(\theta)$  limit the presently allowed vorticity and peculiar velocities to  $(\omega/H)_0 < 7 \times 10^{-7}$  and  $(u)_0 < 10^{-7}$  (in units of  $c$ ).

definite handedness and an observer looking at the centre of the pattern would see a left-handed spiral (Barrow & Silk 1983) – we transform to the true observing angles  $(\theta_{\text{ob}}, \phi_{\text{ob}}) = (\pi - \theta_0, \pi + \theta_0)$  to determine this. The value of the constant  $x$  determines the angular separation between successive twists. When  $x \rightarrow \infty$  we regain the type I quadrupole.

In Figs 4–6 we display the results of calculating the correlation function  $W(\theta)$  for various models.\* Fig. 4 displays  $W(\theta)$  for the VII<sub>0</sub> model with  $x = 0.067$ . Figs 5 and 6 give the open

\* We consider the contribution of the first 100 components in the multipole expansion ( $l \leq 100$ ) to  $W(\theta)$ .

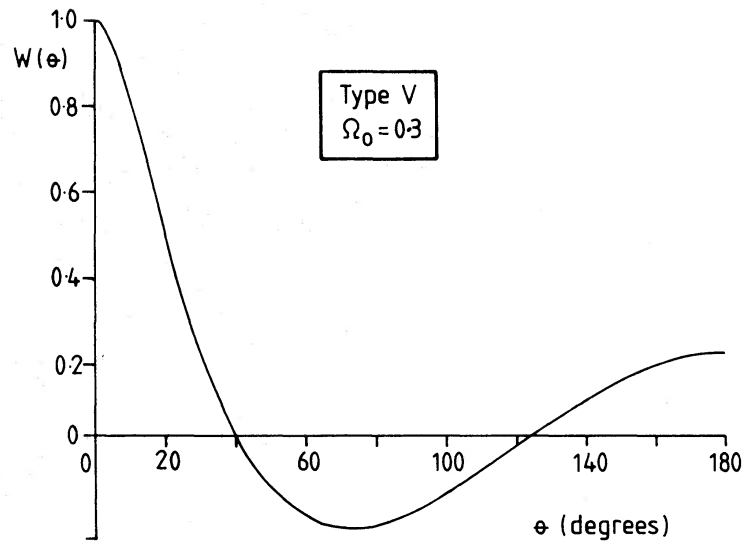


**Figure 6.** The unsmoothed correlation function,  $W(\theta)$ , as Figs 4 and 5, for a type V universe with  $\Omega_0 = 0.3$ . The observational limits on  $W(\theta)$  bound the presently allowed vorticity and peculiar velocities by  $(\omega/H)_0 < 5 \times 10^{-9}$  and  $(u)_0 < 10^{-8}$  (in units of  $c$ ).

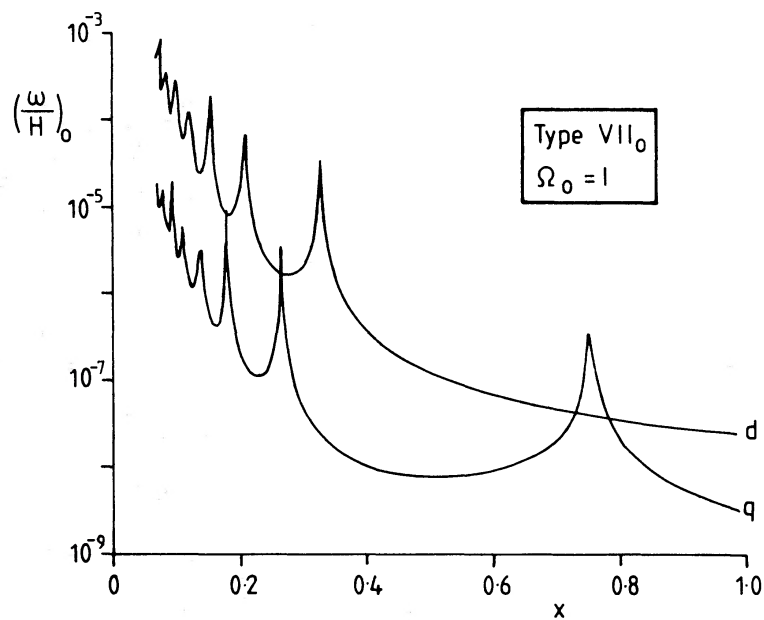


**Figure 7.** Upper limits on the present value of the vorticity parameter  $(\omega/H)_0$ , compatible with observations of the dipole (d) and quadrupole (q) observations of the microwave background in the type VII<sub>0</sub> universe ( $\Omega_0 = 1$ ) as a function of  $x < 1$ ; realistic models have  $x \geq 0.04$ , see equation (3.2). The quasi-periodic behaviour of the curves is a consequence of the geodesic spiralling effect which is more pronounced as  $x \rightarrow 0$ . Precise numerical limits from this plot are given in Table 3.

type VII<sub>h</sub> correlation function in the case  $\Omega_0 = 0.7$  and the type V correlation function when  $\Omega_0 = 0.3$  (see figure captions for details). The limits on rotation given in the captions, which are derived from  $W(\theta)$ , differ slightly from those obtainable from the dipole and quadrupole observations alone (Tables 1–4). In the high density case shown in Fig. 6, it is

virtually a pure quadrupole together with a dipole associated with the rotational velocity effects, whereas in Fig. 5 this pattern has been focused by the negative curvature into a hotspot.

In Figs 7–9 we display the largest values of the vorticity parameter  $(\omega/H)_0$ , that are compatible with the observed limits on the dipole (d) moment and quadrupole (q) moment of the microwave background radiation: these we take as  $a_1 \leq 10^{-3}$  and  $a_2 < 7 \times 10^{-5}$  (Fixsen *et al.* 1983; Lubin *et al.* 1983). Fig. 7 shows the upper limits on  $(\omega/H)_0$  as a function of  $x$  in the VII<sub>0</sub> model where  $\Omega_0 = 1$ . Fig. 8 shows upper limits on  $(\omega/H)_0$  in type VII<sub>h</sub> models with  $\Omega_0 = 0.1$  as  $x$  varies. Fig. 9 shows the variation of the upper limit on

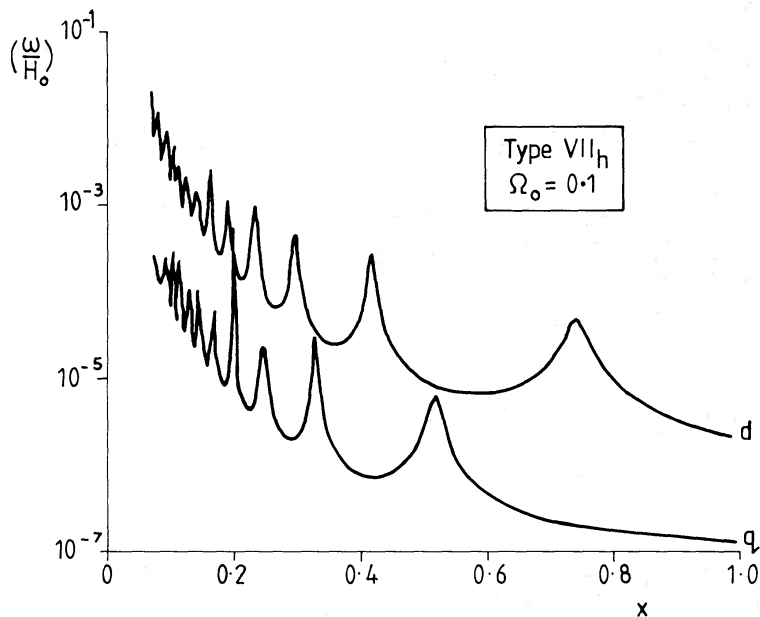


**Figure 8.** As Fig. 7 but showing the upper limits on  $(\omega/H)_0$  in a type VII<sub>h</sub> universe with  $\Omega_0 = 0.1$  for various  $x < 1$ . Precise numerical limits from this plot are given in Table 4.

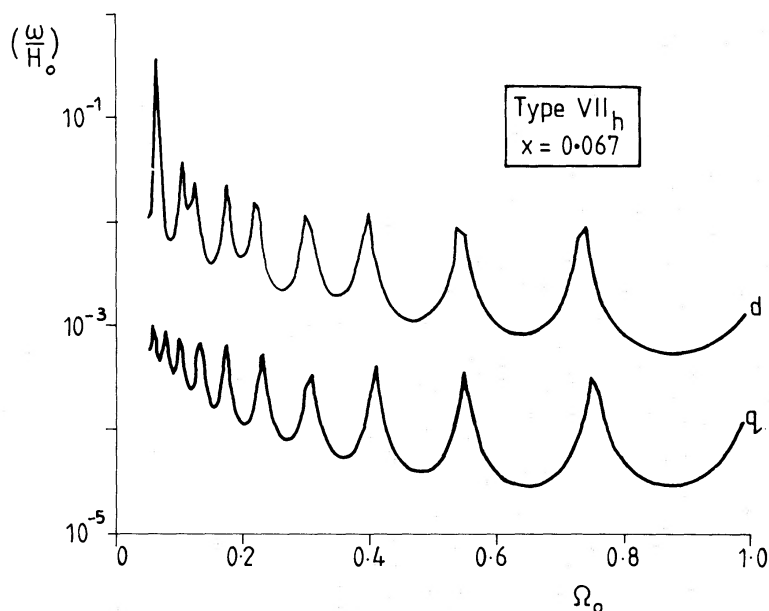


**Figure 9.** As Fig. 6 and 7 but showing upper limits on  $(\omega/H)_0$  in a type VII<sub>h</sub> universe with  $x = 0.067$  as a function of the total present density,  $\Omega_0$ . Precise numerical limits from this plot are given in Table 2.

$(\omega/H)_0$  with  $\Omega_0$  for  $x = 0.067$ . The  $\Omega_0 \rightarrow 1$  limits reduce to those of the VII<sub>0</sub> model with the same value of  $x$ .

Two things are apparent from these figures: first, by using upper limits on the quadrupole fluctuations in the background radiation we can considerably improve earlier limits calculated using the dipole term alone. Secondly, the geodesic spiralling creates oscillatory behaviour in the multiple moments that then shows up in the upper limits. For comparison we show, in Fig. 10, the upper limits on the present value of  $(\omega/H)_0$  as a function of  $\Omega_0$  in Bianchi type V obtained by letting  $x \rightarrow \infty$  in the VII<sub>h</sub> models above. In this limit the geodesic spiralling effect disappears. As  $\Omega_0 \rightarrow 1$  in type V we see that  $(\omega/H)_0 \rightarrow 0$  because vorticity is excluded from Bianchi I models by geometrical effects and therefore upper limits on  $(\omega/H)_0$  obtained using the type V models (Hawking 1969; Batakis & Cohen 1975; Ruzmaikin & Ruzmaikina 1969) are rather misleading when  $\Omega_0 \gtrsim 0.1$ : the vorticity is forced to assume low values by artificial constraints imposed by the fact that the geometry is not the most general homogeneous perturbation of an open Friedmann universe model. The VII<sub>h</sub> limits as  $\Omega_0 \rightarrow 1$  do not suffer from this defect for  $x < 1$ , and smoothly approach the vortical VII<sub>0</sub> model. However, the geometrical suppression of vorticity would occur in the limit  $x \rightarrow \infty$  when we regain type I from type VII<sub>0</sub>. Since the limits we give on  $(\omega/H)_0$  today are based upon the observed dipole and quadrupole components, the best limits are expected in models which possess a pure quadrupole variation, i.e. the cases with  $\Omega_0 \rightarrow 1$  and  $x \rightarrow \infty$ . This sheds light upon the general trends seen in the results figured above. As  $\Omega_0$  falls there is an enhanced focusing effect and the pattern contains more high-order spherical harmonic components and the limits obtained on rotation are weaker. Likewise, if  $x$  is small the tightly wound spiral pattern is not well represented by either a dipole or a quadrupole. The type VII<sub>h</sub> limits are the weakest because of the simultaneous effects of spiralling and focusing for small  $x$  and small  $\Omega_0$ . The quasi-periodic changes in the components of the spherical harmonic expansion as  $\Omega_0$  and  $x$  vary also explains the sensitivity of the limits on  $(\omega/H)_0$  to small changes in the parameters. From equation (4.24) one sees that the general trends in the upper limits are

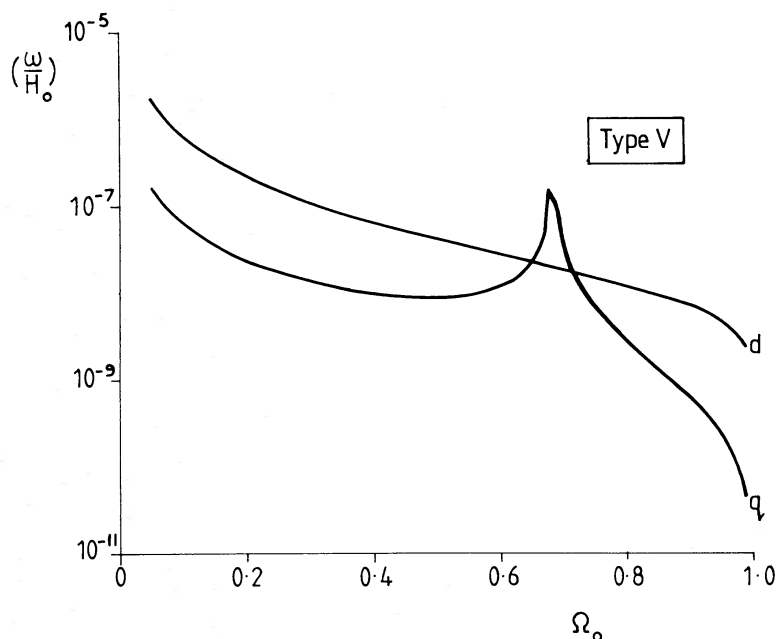


**Figure 10.** As Figs 7, 8 and 9 but giving upper limits on  $(\omega/H)_0$  in type V universes for  $\Omega_0$  in the range 0.05 to 1. The limits approach zero as  $\Omega_0 \rightarrow 1$  for geometrical reasons (see text). Precise numerical limits from this plot are given in Table 1.

**Table 1.** The maximum present vorticity parameter,  $(\omega/H)_0$ , and associated peculiar velocity,  $(u)_0$  in units of  $c$ , allowed by observations of the dipole ( $a_1$ ) and quadrupole ( $a_2$ ) components of the microwave background anisotropy in Bianchi type V universes with different values of the total density  $\Omega_0$ .

$\Omega_0$	Dipole limits		Quadrupole limits	
	$u_0$	$(\omega/H)_0$	$u_0$	$(\omega/H)_0$
0.05	$3.5 \times 10^{-6}$	$1.7 \times 10^{-6}$	$3.4 \times 10^{-7}$	$1.7 \times 10^{-7}$
0.1	$1.3 \times 10^{-6}$	$6.2 \times 10^{-7}$	$1.3 \times 10^{-7}$	$6.2 \times 10^{-8}$
0.2	$4.7 \times 10^{-7}$	$2.1 \times 10^{-7}$	$5.2 \times 10^{-8}$	$2.3 \times 10^{-7}$
0.3	$2.6 \times 10^{-7}$	$1.1 \times 10^{-7}$	$3.2 \times 10^{-8}$	$1.3 \times 10^{-8}$
0.4	$1.6 \times 10^{-7}$	$6.3 \times 10^{-8}$	$2.6 \times 10^{-8}$	$9.9 \times 10^{-9}$
0.5	$1.2 \times 10^{-7}$	$4.1 \times 10^{-8}$	$2.5 \times 10^{-8}$	$8.9 \times 10^{-9}$
0.6	$8.6 \times 10^{-8}$	$2.7 \times 10^{-8}$	$3.6 \times 10^{-8}$	$1.1 \times 10^{-8}$
0.7	$6.7 \times 10^{-8}$	$1.8 \times 10^{-8}$	$1.3 \times 10^{-7}$	$3.5 \times 10^{-8}$
0.8	$5.4 \times 10^{-8}$	$1.2 \times 10^{-8}$	$1.1 \times 10^{-8}$	$2.6 \times 10^{-9}$
0.9	$4.5 \times 10^{-8}$	$7.2 \times 10^{-9}$	$3.6 \times 10^{-9}$	$5.6 \times 10^{-10}$
0.98	$4.2 \times 10^{-8}$	$3.0 \times 10^{-9}$	$1.0 \times 10^{-9}$	$7.1 \times 10^{-11}$

**Table 2.** As Table 1 but for Bianchi VII<sub>h</sub> universes with  $x = 0.067$ .

$\Omega_0$	Dipole limits		Quadrupole limits	
	$u_0$	$(\omega/H)_0$	$u_0$	$(\omega/H)_0$
0.05	$1.1 \times 10^{-3}$	$1.03 \times 10^{-2}$	$6.1 \times 10^{-5}$	$5.8 \times 10^{-4}$
0.1	$1.6 \times 10^{-3}$	$1.5 \times 10^{-2}$	$7.7 \times 10^{-5}$	$7.3 \times 10^{-4}$
0.2	$4.9 \times 10^{-4}$	$4.6 \times 10^{-3}$	$1.2 \times 10^{-5}$	$1.1 \times 10^{-4}$
0.3	$1.2 \times 10^{-3}$	$1.1 \times 10^{-2}$	$2.7 \times 10^{-5}$	$2.5 \times 10^{-4}$
0.4	$1.2 \times 10^{-3}$	$1.1 \times 10^{-2}$	$2.0 \times 10^{-5}$	$1.7 \times 10^{-4}$
0.5	$1.5 \times 10^{-4}$	$1.3 \times 10^{-3}$	$4.6 \times 10^{-6}$	$4.2 \times 10^{-5}$
0.6	$1.2 \times 10^{-4}$	$1.0 \times 10^{-3}$	$4.4 \times 10^{-6}$	$3.9 \times 10^{-5}$
0.7	$1.7 \times 10^{-4}$	$1.5 \times 10^{-3}$	$4.6 \times 10^{-6}$	$4.0 \times 10^{-5}$
0.8	$9.6 \times 10^{-5}$	$8.2 \times 10^{-4}$	$5.4 \times 10^{-6}$	$4.6 \times 10^{-5}$
0.9	$6.6 \times 10^{-5}$	$5.4 \times 10^{-4}$	$3.6 \times 10^{-6}$	$3.0 \times 10^{-5}$
0.98	$1.4 \times 10^{-4}$	$1.3 \times 10^{-3}$	$1.1 \times 10^{-5}$	$8.5 \times 10^{-5}$

**Table 3.** As Table 1 but for Bianchi VII<sub>0</sub> universes ( $\Omega_0 = 1$ ) for a range of values of the constant parameter  $x$ .

$x$	Dipole limits		Quadrupole limits	
	$u_0$	$(\omega/H)_0$	$u_0$	$(\omega/H)_0$
0.07	$6.6 \times 10^{-5}$	$4.7 \times 10^{-4}$	$2.7 \times 10^{-6}$	$1.9 \times 10^{-5}$
0.1	$5.9 \times 10^{-5}$	$2.9 \times 10^{-4}$	$6.0 \times 10^{-7}$	$3.0 \times 10^{-6}$
0.2	$5.6 \times 10^{-6}$	$1.4 \times 10^{-5}$	$8.0 \times 10^{-8}$	$2.0 \times 10^{-7}$
0.3	$1.2 \times 10^{-6}$	$2.1 \times 10^{-6}$	$2.9 \times 10^{-8}$	$4.8 \times 10^{-8}$
0.4	$3.1 \times 10^{-7}$	$3.8 \times 10^{-7}$	$8.6 \times 10^{-9}$	$1.1 \times 10^{-8}$
0.5	$1.2 \times 10^{-7}$	$1.2 \times 10^{-7}$	$7.9 \times 10^{-9}$	$7.9 \times 10^{-9}$
0.6	$8.0 \times 10^{-8}$	$6.7 \times 10^{-8}$	$1.1 \times 10^{-8}$	$9.2 \times 10^{-9}$
0.7	$6.4 \times 10^{-8}$	$4.6 \times 10^{-8}$	$3.0 \times 10^{-8}$	$2.1 \times 10^{-8}$
0.8	$5.6 \times 10^{-8}$	$3.5 \times 10^{-8}$	$3.2 \times 10^{-8}$	$2.0 \times 10^{-8}$
0.9	$5.1 \times 10^{-8}$	$2.8 \times 10^{-8}$	$1.0 \times 10^{-8}$	$5.6 \times 10^{-9}$
1.0	$4.8 \times 10^{-8}$	$2.4 \times 10^{-8}$	$6.3 \times 10^{-9}$	$3.2 \times 10^{-9}$

**Table 4.** As Table 3 but for Bianchi VII<sub>h</sub> universes with  $\Omega_0 = 0.1$ .

$x$	Dipole limits		Quadrupole limits	
	$u_0$	$(\omega/H)_0$	$u_0$	$(\omega/H)_0$
0.07	$2.3 \times 10^{-3}$	$2.1 \times 10^{-2}$	$2.9 \times 10^{-5}$	$2.7 \times 10^{-4}$
0.1	$2.7 \times 10^{-4}$	$1.8 \times 10^{-3}$	$9.5 \times 10^{-6}$	$6.5 \times 10^{-5}$
0.2	$6.3 \times 10^{-5}$	$2.5 \times 10^{-4}$	$1.4 \times 10^{-4}$	$5.4 \times 10^{-4}$
0.3	$1.6 \times 10^{-4}$	$4.4 \times 10^{-4}$	$7.7 \times 10^{-7}$	$2.1 \times 10^{-6}$
0.4	$2.4 \times 10^{-5}$	$4.9 \times 10^{-5}$	$3.7 \times 10^{-7}$	$7.5 \times 10^{-7}$
0.5	$5.0 \times 10^{-6}$	$9.3 \times 10^{-6}$	$1.4 \times 10^{-6}$	$2.3 \times 10^{-6}$
0.6	$5.1 \times 10^{-6}$	$6.7 \times 10^{-6}$	$3.5 \times 10^{-7}$	$4.6 \times 10^{-7}$
0.7	$1.5 \times 10^{-5}$	$1.6 \times 10^{-5}$	$2.0 \times 10^{-7}$	$2.2 \times 10^{-7}$
0.8	$9.6 \times 10^{-6}$	$9.0 \times 10^{-6}$	$1.7 \times 10^{-7}$	$1.6 \times 10^{-7}$
0.9	$4.0 \times 10^{-6}$	$3.2 \times 10^{-6}$	$1.7 \times 10^{-7}$	$1.4 \times 10^{-7}$
1.0	$2.8 \times 10^{-6}$	$2.0 \times 10^{-6}$	$1.7 \times 10^{-7}$	$1.2 \times 10^{-7}$

caused by the  $f(x, \theta_0)$  components of  $A(\theta_0)$  and  $B(\theta_0)$ , whereas the quasi-periodic variations are created by the  $\sin, \cos [(2 \cos \theta_0)/x]$  variations. The difference between the limits that can be placed on  $(\omega/H)_0$  from the dipole and quadrupole observations arise primarily from the different magnitudes of the observational data ( $a_1 \leq 10^{-3}$ ,  $a_2 < 7 \times 10^{-5}$ ). However, even if  $a_1$  and  $a_2$  were equal, the limit on  $(\omega/H)_0$  derived from  $a_2$  will still be slightly stronger. When comparing our limits with those of Collins & Hawking (1973) it should be noted that for Bianchi types V and VII<sub>h</sub> they take  $\Omega_0 = 10^{-2}$  throughout. We do not consider here the case of last scattering occurring at low redshift ( $1 + z_E \sim 10$ ) because of reheating since observations over angular scales exceeding that subtending the particle horizon at  $z_E \sim 9$ ,  $\theta \gtrsim 5 \Omega_0^{1/3}$ , will measure anisotropies unaffected by moderate reheating, but see Section 6.

In Tables 1–4 we summarize the upper limits on the present vorticity to Hubble rate  $(\omega/H)_0$ , and the associated peculiar velocity scalar,  $(u)_0$ , imposed by the dipole and quadrupole observations in the flat and open universes we have examined.

## 5 Closed universes

The most general spatially homogeneous universe model that contains the closed Friedmann model as a particular case is that of Bianchi type IX. We shall linearize the Einstein equations for the type IX model about the Friedmann model as we did for the type VII models about the open Friedmann models. However, the situation turns out to be more complicated than was the case in the type VII<sub>o</sub> and VII<sub>h</sub> universes. There exist three non-zero velocity components  $u_i$ , which are not related to the induced shear in a straightforward manner. The closed Friedmann background universe is described by

$$e^\alpha = \frac{1}{2} e^{\alpha_m} (1 - \cos \tau) \equiv \frac{dt}{d\tau}, \quad (5.1)$$

with present value of the scale factor given by

$$e^{\alpha_0} = H_0^{-1} (\Omega_0 - 1)^{-1/2}. \quad (5.2)$$

The scale-factor at the moment of maximum expansion,  $\tau_m$ , is denoted by  $\alpha_m$  and

$$e^{\alpha_m} = \Omega_0 H_0^{-1} (\Omega_0 - 1)^{-3/2}. \quad (5.3)$$

One can show (see Appendix B), that the dependence of the velocity components,  $u_i$ , on the shear tensor is given by a complicated expression of the form (B.12)–(B.14)

$$u_i \propto \epsilon_{ABi} \left\{ \frac{\sigma_{j[B}^{(G)} \sigma_{A]j}^{(D)}}{H^2} \right\}_0 \quad (5.4)$$

where  $[B, A] \equiv \frac{1}{2}(BA - AB)$  denotes index antisymmetrization and the shear consists of growing (G) and decaying (D) modes. The most general models with vorticity have all three  $u_i$  components non-zero. Nevertheless, the geodesics propagate in a particularly simple fashion along the  $\theta$  and  $\phi$  directions with no focusing and no spiralling (see A.11).

For type IX universes the temperature anisotropy, given in general by the master equation (2.18), simplifies to

$$\frac{\Delta T}{T_0} = p^i [(u_i)_0 - (u_i)_E] - p^j p^k (\beta_0 - \beta_E)_{jk}. \quad (5.5)$$

If the radiation was emitted at a large redshift,  $z_E$ , then  $(u_i)_0$  is negligible compared to  $(u_i)_E$  and if  $(\Omega_0 - 1) \Omega_0^{-1}$  is small compared to unity then we have that

$$\frac{\Delta T}{T_0} \approx -p^i (u_i)_E - p^j p^k Q_{jk} \quad (5.6)$$

where  $(u_i)_E$  reduces, in this approximation, using (B.14), to

$$(u_i)_E \approx \frac{5}{24} \epsilon_{ABi} \left\{ \frac{\sigma_{j[B}^{(G)} \sigma_{A]j}^{(D)}}{H^2} \right\}_0 \left( \frac{\Omega_0}{\Omega_0 - 1} \right)^{1/2} z_E \quad (5.7)$$

and the quadrupole distortion tensor,  $Q_{ij}$ , is just the matrix

$$Q_{ij} \equiv (\beta_0 - \beta_E)_{jk} \quad (5.8)$$

which, from Appendix B equations (B.6–10), is calculated to be

$$Q_{ij} = \left( \frac{\sigma_{ij}^{(G)}}{H} \right)_0 [1 - (1 + z_E)^{-1}] + \frac{2}{3} \left( \frac{\sigma_{ij}^{(D)}}{H} \right)_0 [(1 + z_E)^{3/2} - 1]. \quad (5.9)$$

The present vorticity is given by

$$\left( \frac{\omega}{H} \right)_0 = \frac{(\Omega_0 - 1)^{1/2}}{2} [(u_1)^2 + (u_2)^2 + (u_3)^2]_0^{1/2} \quad (5.10)$$

where the  $u_i$  are given in Appendix B by equations (B.12)–(B.14). Unlike in the open and flat universes discussed in Section 4, the closed universe does not admit a simple relationship between the vorticity and the induced shear; the best that can be done is the system (5.10) and (B.13).\*

Since  $Q_{ij}$  is a traceless symmetric matrix we can expand (5.6) using the explicit forms of the direction cosines  $p^i$  to give

$$\begin{aligned} \frac{\Delta T}{T_0} = & -(u_1)_E \cos \theta - (u_2)_E \sin \theta \cos \phi - (u_3)_E \sin \theta \sin \phi \\ & + \frac{Q_{11}}{2} (1 - 3 \cos^2 \theta) - \frac{1}{2} \sin^2 \theta \cos 2\phi (Q_{22} - Q_{33}) \\ & - \sin 2\theta (Q_{12} \cos \phi + Q_{13} \sin \phi) - Q_{23} \sin^2 \theta \sin 2\phi. \end{aligned} \quad (5.11)$$

\* Whereas our calculation in Section 4 calculated only the distortions to the temperature profile contributed by the vorticity, for type IX we shall consider the general form of the distortions due to shear and rotation because they are intertwined in this case.

Now, using (2.5), we can calculate the dipole and quadrupole coefficients in the spherical harmonic expansion of (5.11). We find\*

$$a_{10} = \left(\frac{4\pi}{3}\right)^{1/2} (u_1)_E = \frac{5}{6} \left(\frac{\pi}{3}\right)^{1/2} \left\{ \frac{\sigma_{j[B}^{(G)} \sigma_{A]j}^{(D)}}{H^2} \right\}_0 \left( \frac{\Omega_0}{\Omega_0 - 1} \right)^{1/2} z_E, \quad (5.12)$$

$$\begin{aligned} a_{1,\pm 1} &= \left(\frac{2\pi}{3}\right)^{1/2} (\mp u_2 + iu_3)_E \\ &= \frac{5}{12} \left(\frac{2\pi}{3}\right)^{1/2} \left\{ \frac{\pm \sigma_{j[3}^{(G)} \sigma_{1]j}^{(D)} + i\sigma_{j[2}^{(G)} \sigma_{1]j}^{(D)}}{H^2} \right\}_0 \left( \frac{\Omega_0}{\Omega_0 - 1} \right)^{1/2} z_E, \end{aligned} \quad (5.13)$$

$$\begin{aligned} a_{20} &= \left(\frac{4\pi}{5}\right)^{1/2} Q_{11} \\ &= \left(\frac{4\pi}{5}\right)^{1/2} \left\{ \left( \frac{\sigma_{11}^{(G)}}{H} \right)_0 [1 - (1 + z_E)^{-1}] \right. \\ &\quad \left. + \frac{2}{3} \left( \frac{\sigma_{11}^{(D)}}{H} \right)_0 [(1 + z_E)^{3/2} - 1] \right\}, \end{aligned} \quad (5.14)$$

$$\begin{aligned} a_{2,\pm 1} &= \left(\frac{8\pi}{15}\right)^{1/2} [\pm Q_{12} - iQ_{13}] \\ &= \left(\frac{8\pi}{15}\right)^{1/2} \left\{ \left[ \frac{\pm \sigma_{12}^{(G)} - i\sigma_{13}^{(G)}}{H} \right]_0 [1 - (1 + z_E)^{-1}] \right. \\ &\quad \left. + \frac{2}{3} \left[ \frac{\pm \sigma_{12}^{(D)} - i\sigma_{13}^{(D)}}{H} \right]_0 [(1 + z_E)^{3/2} - 1] \right\}, \end{aligned} \quad (5.15)$$

$$\begin{aligned} a_{2,\pm 2} &= \left(\frac{8\pi}{15}\right)^{1/2} \left[ \frac{1}{2} (Q_{33} - Q_{22}) \pm iQ_{23} \right] \\ &= \left(\frac{8\pi}{15}\right)^{1/2} \left[ \left\{ \frac{1/2 (\sigma_{33}^{(G)} - \sigma_{22}^{(G)}) \pm i\sigma_{23}^{(G)}}{H} \right\}_0 [1 - (1 + z_E)^{-1}] \right. \\ &\quad \left. + \frac{2}{3} \left\{ \frac{1/2 (\sigma_{33}^{(D)} - \sigma_{22}^{(D)}) \pm i\sigma_{23}^{(D)}}{H} \right\}_0 [(1 + z_E)^{3/2} - 1] \right]. \end{aligned} \quad (5.16)$$

Hence, using (4.20), we find the dipole and quadrupole moments,  $a_1$  and  $a_2$ , to be

$$a_1 = \left[ \frac{(u_1)^2 + (u_2)^2 + (u_3)^2}{3} \right]_E^{1/2} = \frac{(u)_E}{\sqrt{3}}, \quad (5.17)$$

$$a_2 = \left(\frac{2}{15}\right)^{1/2} (Q_{ij}Q_{ij})^{1/2}, \quad (5.18)$$

\* We include several corrections to expressions obtained by Fabbri, Pucacco & Ruffini (1984).

where the  $u_i$  and  $Q_{ij}$  are given explicitly by (5.7) and (5.9). Equations (B.13) and (B.14) relate the velocity scalars,  $(u)_0$  to  $(u)_E$  through

$$(u)_0 = \left( \frac{1 + z_E}{1 + \Omega_0 z_E} \right)^{1/2} \frac{(16 - 13\Omega_0)(u)_E}{(16 - 13\Omega_0 + 3\Omega_0 z_E)} \quad (5.19)$$

so

$$(u)_0 \approx \frac{(1 + z_E)^{1/2}}{(1 + \Omega_0 z_E)^{3/2}} (u)_E. \quad (5.20)$$

Observational limits on the dipole moment,  $a_1$ , give us an upper limit on the present velocity when we use (5.19) and take  $1 + z_E = 10^3$  because we have

$$(u)_0 = \frac{\sqrt{3}(1 + z_E)^{1/2} a_1}{(1 + \Omega_0 z_E)^{3/2}}. \quad (5.21)$$

Equation (5.10) gives a limit on the vorticity parameter  $(\omega/H)_0$  in terms of any limit on  $a_1$  since we have that

$$\left( \frac{\omega}{H} \right)_0 = \frac{\sqrt{3}(\Omega_0 - 1)^{1/2} (1 + z_E)^{1/2} a_1}{(1 + \Omega_0 z_E)^{3/2}} \quad (5.22)$$

$$\approx \frac{\sqrt{3}(\Omega_0 - 1)^{1/2} a_1}{2(1 + \Omega_0 z_E)}. \quad (5.23)$$

We see that the limit on the velocity scalar, (5.21), is virtually independent of  $\Omega_0 \approx 1$ . For  $1 + z_E = 10^3$  and  $a_1 \leq 10^{-3}$ , as observed, we calculate therefore the maximum present velocity and vorticity compatible with the *dipole* observations to be

$$(u)_0 \leq 1.7 \times 10^{-6} \quad (5.24)$$

$$\left( \frac{\omega}{H} \right)_0 \leq 8 \times 10^{-7} (\Omega_0 - 1)^{1/2} \quad (5.25)$$

when  $\Omega_0$  is close to unity.

We would expect that other limits on  $(u)_0$  and  $(\omega/H)_0$ , derived from the observational upper limits on the *quadrupole* component of the background radiation of  $a_2 < 7 \times 10^{-5}$  would considerably strengthen (5.24) and (5.25). However, the observational limit on  $a_2$  is not so easily related to the present vorticity because the dependence of  $Q_{ij}$  on the shear differs from that of the velocities; therefore, we can obtain order of magnitude estimate only. Using (5.18), we know that if the decaying mode were zero ( $\sigma_{ij}^{(D)} \equiv 0$ ) in (5.9) then we have the inequality

$$\left\{ \frac{\sigma_{ij}^{(G)} \sigma_{ij}^{(G)}}{H^2} \right\}_0 [1 - (1 + z_E)^{-1}] < \left( \frac{15}{2} \right)^{1/2} a_2 \quad (5.26)$$

whereas if we set the growing shear mode,  $\sigma_{ij}^{(G)}$ , equal to zero then the corresponding limit is

$$\frac{2}{3} \left\{ \frac{\sigma_{ij}^{(D)} \sigma_{ij}^{(D)}}{H^2} \right\}_0 [(1 + z_E)^{3/2} - 1] < \left( \frac{15}{2} \right)^{1/2} a_2. \quad (5.27)$$

The velocity scalar today has the form, (B.13),

$$(u)_0 = \frac{5(16 - 13\Omega_0)}{36\Omega_0(\Omega_0 - 1)^{1/2}} \times \left\{ \text{antisymmetric terms like } \left( \frac{\sigma_j^{(G)} \sigma_A^{(D)}}{H^2} \right)_j \right\} \quad (5.28)$$

$$< \frac{5(16 - 13\Omega_0)}{36\Omega_0(\Omega_0 - 1)^{1/2}} \left\{ \frac{45(a_2)^2}{4[(1 + z_E)^{3/2} - 1]} \right\} \quad (5.29)$$

$$\lesssim \frac{5(a_2)^2}{(\Omega_0 - 1)^{1/2} z_E^{3/2}}. \quad (5.30)$$

Hence, for last scattering at  $1 + z_E = 10^3$  the observational upper bound on  $a_2$  of  $7 \times 10^{-5}$  gives very powerful upper limits on the present velocity and vorticity [from (5.30) and (5.10)] of

$$(u)_0 < 7.8 \times 10^{-13} (\Omega_0 - 1)^{-1/2}, \quad (5.31)$$

$$\left( \frac{\omega}{H} \right)_0 < 3.9 \times 10^{-13}. \quad (5.32)$$

These limits are nearly two orders of magnitude stronger than those given earlier by less detailed analyses (Collins & Hawking 1973). They show that a closed, approximately Friedmannian universe can have rotated through less than  $4 \times 10^{-6}$  seconds of arc since the expansion began. We notice that the type IX limits with  $\Omega_0$  very close to unity are not the same as the VII<sub>0</sub> vorticity limits unless the parameter  $x$  is chosen to have a specially large value. One might have expected that the VII<sub>0</sub> and IX limits on the vorticity would have been comparable when  $x = 1$  in type VII<sub>0</sub> but we can see from Table 3 that, when  $x = 1$  the VII<sub>0</sub> limit is  $(\omega/H)_0 \lesssim 3.2 \times 10^{-9}$ , considerably weaker than that in type IX given by (5.32). We note also that the limit (5.32) is independent of  $\Omega_0$  when  $\Omega_0$  is close to unity (see equation B.7), but the limit imposed by the dipole temperature fluctuations (5.25) is proportional to  $(\Omega_0 - 1)^{1/2}$ . In view of the possibility that our Universe may well possess a value  $\Omega_0 = 1 \pm \epsilon$  where  $\epsilon \geq 0$  is very small it is extremely interesting that there appears to exist a large discrete difference in the level of vorticity compatible with a given amplitude of background radiation fluctuation in universes with  $\Omega_0 = 1 + \epsilon$  and  $\Omega_0 = 1 - \epsilon$  as  $\epsilon \rightarrow 0$ . It may be possible to determine observationally whether a Friedmann universe is open or closed no matter how close  $\Omega_0$  is to unity. For example, the detection of the spiral geodesic effect described in Section 4 would enable us to distinguish a flat universe with  $\Omega_0 = 1$  from a closed universe with  $\Omega_0 = 1 + \epsilon$ ,  $\epsilon > 0$  *no matter how small the value of  $\epsilon$* , because the spiral effect will not occur in a closed universe. This is interesting if only because it is often claimed that we will never be able to tell whether the Universe is open or closed if  $\Omega_0$  is arbitrarily close to unity. Of course, if the anisotropy and vorticity modes we have been studying in this paper have very small amplitudes their contribution to  $\Delta T/T_0$  will be undetectably small. If 'inflation' occurs in the way predicted by simple models then this should predict that no large-scale rotation exists.

## 6 Effects of smoothing

The temperature distributions and correlation functions derived in Sections 5 and 6 are those that would be found by ideal measuring devices. However, in practice, detectors have a finite beamwidth which allows the signal to be contaminated from other directions. If the beamwidth is  $\Delta_A$  then this will lead to significant effects on  $W(\theta)$  on angular scales  $\theta \lesssim \Delta_A$ .

Bajtlik *et al.* (1985) have examined this effect in detail using the Gaussian convolution outlined in equations (2.20)–(2.22). They find the peak in  $W(\theta)$  at small angles,  $\theta \lesssim \Delta_A$  seen in Figs 4–6, to be reduced and slightly broadened. Typical values of  $\Delta_A$  are of order  $7^\circ$  and for this choice the reduced quadrupole moment,  $\bar{a}_2$ , calculated from the smoothed correlation function,  $\bar{W}(\theta)$ , differs from the  $a_2$  calculated from  $W(\theta)$  by less than 5 per cent. The effects of reionization of the universe at a redshift  $z_*$  such that the optical depth is unity at  $z_*$  erases fluctuations in  $\Delta T/T_0$  on angular scales less than that subtending the horizon at  $z_*$ , that is less than  $\Delta_R = 15\Omega_0^{1/3}$  degrees (Bajtlik *et al.* 1985). The effects are found by Bajtlik *et al.* to be similar in character but slightly less significant than those of finite beam-width. Both effects can be well accounted for by convolving the unsmoothed predicted patterns with a Gaussian of half-width  $(\Delta_R^2 + \Delta_A^2)^{1/2}$ , equations (2.20–2.21).

Both of the above effects have negligible effects upon our conclusions since they produce effects on scales  $\theta \lesssim (\Delta_R^2 + \Delta_A^2)^{1/2} \lesssim 16^\circ$ . The dipole and quadrupole components are not strongly affected by smoothing over these scales and hence our limits on vorticity are essentially unaffected. Also, the limits given in the captions of Figs 4–6 derived from  $W(\theta)$  were derived from observations of the correlation function for  $\theta > 10^\circ$  and should be essentially unchanged by smoothing effects. The reheating considered above, with unit optical depth  $\tau$ , for Thomson scattering arising at a redshift  $z_*$  due to reheating of the cosmic medium, are moderate. The case of strong reheating has been considered by Negroponte & Silk (1980). They find that when reionization at  $z_*$  leads to  $\tau(z_*) \gg 1$  then smoothing of large-scale anisotropy occurs. [This was also assumed by Collins & Hawking (1973).] However, a saturation of the damping effect is attained when  $\tau(z_*) \sim 30$  and further increase of  $\tau$  does not deplete the residual anisotropy by a significant factor. In order to attain an optical depth,  $\tau$ , due to electron scattering when the present density of ionized gas is  $\Omega_g$  (we assume the *total* density  $\Omega_0 = 1$ ; this is the most favourable case  $H_0 = 100 \text{ km s}^{-1} \text{ Mpc}^{-1}$ ) then one must ionize the Universe at a redshift

$$1 + z_* \gtrsim 613 \left(\frac{\tau}{30}\right)^{2/3} \left(\frac{0.05}{\Omega_g}\right)^{2/3}. \quad (6.1)$$

Nucleosynthesis of helium and deuterium (Pagel 1983) limits the total baryon density in the Universe, and hence the gas density, to  $0.01 \lesssim \Omega_g \lesssim 0.05$  (Yang *et al.* 1984). The major component of a universe containing  $\Omega_0 \sim 1$  would have to be in a non-baryonic form which plays no role in the thermal history and rescattering of the background radiation. If (6.1) holds, then the anisotropies in the background radiation due to shear and vorticity would evolve as though isotropic until a redshift  $z_1$  where  $\tau(z_1) = 1$  determines  $z_1$ .

The most favourable case for reheating,  $\Omega_0 \sim 1$ , gives

$$1 + z_1 \sim 60 \left(\frac{0.05}{\Omega_g}\right)^{2/3} \quad (6.2)$$

and this results in a weakening of the limits calculated on the cosmic vorticity in Sections 4 and 5 from the dipole, quadrupole and correlation functions by at most a factor  $\sim 50$ . This factor can also be seen in some numerical results of Bajtlik *et al.* (1985). If  $\Omega_0 < 1$  the effects of a strong reheating are less significant.

## 7 Conclusions

We have provided a detailed analysis of the angular variations to be expected in the microwave background radiation if the universe contains small homogeneous anisotropies. Where

previous investigations have concentrated upon calculating bounds on the amplitudes of the allowed anisotropic distortions we have given detailed predictions of the angular variations expected on the sky together with the angular correlation functions. We have also indicated the effects of beam-smoothing and reionization of the cosmic medium. In addition to the 'hotspot' effect found in open universes and discussed earlier (Barrow *et al.* 1983), we have calculated the details of the geodesic spiralling that occurs in the most general flat and open Bianchi-type universe models. These models are parametrized by a constant,  $x$ , which measures the characteristic pitch angle of the spiralling on the sky.

We used these analyses to calculate the maximum level of homogeneous vorticity that is permitted in the Universe by the current observations of the microwave background dipole and quadrupole moments. Previous analyses had used only the dipole limits whereas present upper limits on the quadrupole moment allow for stronger limits to be placed on the level of any cosmic vorticity.

Recent studies of the position angles and polarization of double radio sources have led to the suggestion that the Universe is rotating with a vorticity to expansion rate ratio of  $(\omega/H)_0 \sim 10^{-3}$  (Birch 1982). This claim is based upon observations of 137 radio sources which display a systematic anisotropy in the value of a measure of the orientations of the major axis of each radio source relative to the polarization of the radio emission. This anisotropy has been found to be statistically highly significant (Kendall & Young 1984), but its status as evidence for large-scale vorticity is ambiguous (Phinney & Webster 1983; Birch 1983). We have found that the current observations of the microwave background permit  $(\omega/H)_0$  to be no larger than  $3.9 \times 10^{-13}$  if the Universe is closed with  $\Omega_0 < 2$ , no larger than  $1.9 \times 10^{-5}$  if it is flat ( $\Omega_0 = 1$ ) and no larger than  $10^{-4}$  if it is open ( $\Omega_0 \geq 0.05$ ). These are the limits for the least favourable choices of the spiralling parameter  $x$ , complete results can be seen in the figures and Tables 1–4. These results indicate that if the effect found by Birch is real it cannot be attributed to cosmic vorticity.

The limits we have found depend strongly on whether the Universe is open or closed. The vorticity modes permitted in closed universes differ significantly from those allowed in flat and open universes and the vorticity level that is compatible with microwave background observations is significantly different in the two cases no matter how close  $\Omega_0$  is to unity. Furthermore, the geodesic spiralling effect occurs only in flat and open universes and its detection would give definite proof that the Universe is not closed. The hotspot effect also allows one to infer that the Universe is open if it is detected, but a significant hotspot focusing requires  $\Omega_0 \leq 0.1$ . It offers no hope as a means of distinguishing between open and closed universe when  $\Omega_0$  is arbitrarily close to unity. However, the spiral effect has the same qualitative form however close  $\Omega_0$  is to unity and only occurs if  $\Omega_0 \leq 1$ .

### Acknowledgments

We would like to thank P. Amsterdamski, S. Bajtlik, P. Birch, C. Frenk, F. Graham Smith, B. Lovell, R. Matzner, J. Silk, J. Stein-Schabes, R. J. Tayler, D. W. Sciama and B. Tolman for discussions. DS was supported by an SERC postgraduate studentship and RJ by an SERC visiting fellowship and DOE grant 84-ER 40161 at Berkeley whilst this work was completed.

### References

- Abbott, L. & Wise, M., 1984. *Astrophys. J.*, **282**, L47.
- Bajtlik, S., Juskiewicz, R., Proszynski, M. & Amsterdamski, P., 1985. *Astrophys. J.*, in press.
- Barrow, J. D., 1977. *Mon. Not. R. astr. Soc.*, **179**, 47P.
- Barrow, J. D., 1978. *Nature*, **272**, 211.

- Barrow, J. D., 1983. In: *The Very Early Universe*, eds Gibbons, G., Hawking, S. W. & Siklos, S. T. C., Cambridge University Press, Cambridge.
- Barrow, J. D., Juszkiewicz, R. & Sonoda, D. H., 1983. *Nature*, **305**, 397.
- Barrow, J. D. & Silk, J., 1983. *The Left Hand of Creation*, Basic Books, New York.
- Barrow, J. D. & Tipler, F. J., 1985. *The Anthropic Cosmological Principle*, Oxford University Press, in Press.
- Barrow, J. D. & Turner, M. S., 1982. *Nature*, **298**, 801.
- Batakis, N. & Cohen, J. M., 1975. *Phys. Rev. D*, **12**, 1544.
- Birch, P., 1982. *Nature*, **298**, 451.
- Birch, P., 1983. *Nature*, **301**, 736.
- Collins, C. B. & Hawking, S. W., 1973. *Mon. Not. R. astr. Soc.*, **162**, 307.
- Doroshkevich, A. G., Lukash, V. N. & Novikov, I. D., 1975. *Soviet Astr.*, **18**, 554.
- Ellis, G. F. R. & King, A., 1974. *Comm. Math. Phys.*, **38**, 119.
- Ellis, J. & Olive, K., 1983. *Nature*, **303**, 679.
- Fabbri, R., Pucacco, G. & Ruffini, R., 1984. *Astr. Astrophys.*, **135**, 53.
- Fixsen, D. J., Cheng, E. S. & Wilkinson, D. T., 1983. *Phys. Rev. Lett.*, **44**, 1563.
- Gibbons, G., Hawking, S. W. & Siklos, S. T. C. (eds), 1983. *The Very Early Universe*, Cambridge University Press, Cambridge.
- Hawking, S. W., 1969. *Mon. Not. R. astr. Soc.*, **142**, 129.
- Hawking, S. W., 1982a. *Phys. Lett.*, **115B**, 295.
- Hawking, S. W., 1982b. *Astrophysical Cosmology*, Pontif. Acad. Scient. Scripta Varia, **48**, 563.
- Kendall, D. G., 1984. *Q. Jl R. astr. Soc.*, **22**, 3.
- Kendall, D. G. & Young, G. A., 1984. *Mon. Not. R. astr. Soc.*, **207**, 637.
- Lubin, P. M., Epstein, G. L. & Smoot, G. F., 1983. *Phys. Rev. Lett.*, **50**, 616.
- Lukash, V. N., Novikov, I. D. & Starobinskii, A. A., 1976. *Soviet Phys.*, **42**, 757.
- MacCallum, M. A. H., 1979. In: *General Relativity: An Einstein Centenary Survey*, eds Hawking S. W. & Israel, W., Cambridge University Press, Cambridge.
- Matzner, R. A. & Tolman, B. W., 1982. *Phys. Rev. D*, **26**, 2951.
- Misner, C. W., 1968. *Astrophys. J.*, **151**, 459.
- Negroponete, J. & Silk, J., 1980. *Phys. Rev. Lett.*, **44**, 1433.
- Pagel, B. E. J., 1983. *Phil. Trans. R. Soc.*, **A310**, 245.
- Penrose, R., 1979. In: *General Relativity: An Einstein Centenary Survey*, eds Hawking, S. W. & Israel, W., Cambridge University Press, Cambridge.
- Phinney, E. S. & Webster, R. L., 1983. *Nature*, **301**, 735.
- Raine, D. J., 1975. *Mon. Not. R. astr. Soc.*, **171**, 507.
- Raine, D. J. & Heller, M., 1981. *The Science of Space-Time*, Pachart, Tucson.
- Ruzmaikin, A. & Ruzmaikina, T. V., 1969. *Soviet Phys.*, **29**, 934.
- Starobinskii, A. A., 1982. *Phys. Lett.*, **117B**, 175.
- Starobinskii, A. A., 1979. *Soviet Phys. Lett.*, **30**, 683.
- Yang, J., Turner, M. S., Steigman, G., Schramm, D. N. & Olive, K. A., 1984. *Astrophys. J.*, **281**, 493.

## Appendix A

Light rays follow null geodesics through space-time. If  $K^\mu$  is the tangent vector to one such geodesic then it satisfies

$$K^\mu_{;\nu} K^\nu = 0. \quad (\text{A.1})$$

In the orthonormal basis of Collins & Hawking we employ, the geodesic equations are

$$\dot{K}_A = C_{CA}^B \frac{K_B K^C}{K^0} \quad (\text{A.2})$$

for a null geodesic

$$K^0 K_0 + K_A K^A = 0 \quad (\text{A.3})$$

but,

$$K_0 = -K^0$$

so

$$K^0 = (K^A K_A)^{1/2}$$

and

$$K_A = g_{AB} K^B = e^{2\alpha} (e^{2\beta})_{AB} K^B \quad (\text{A.4})$$

with  $K_A = (K \cos \theta, K \sin \theta \cos \phi, K \sin \theta \sin \phi)$  where  $K$  is constant. For small anisotropies  $g_{AB} \approx e^{2\alpha} \delta_{AB}$  and  $K^0 \approx K e^{-\alpha}$ ; the geodesic equations then reduce, to first order, to

$$\dot{K}_A = \frac{1}{K} C_{CA}^B K_B K_C e^{-\alpha}. \quad (\text{A.5})$$

Introducing a new time by  $d/d\tau = e^\alpha d/dt \equiv (\prime)$  we have

$$K'_A = C_{CA}^B K_B K_C K^{-1}. \quad (\text{A.6})$$

If we use the values of the structure constants for Bianchi types I, V, VII<sub>o</sub>, VII<sub>h</sub> and IX, which are those containing Friedmann models as special isotropic cases, the equations and their solutions are given as follows:

*Bianchi type I*

$$\theta' = \phi' = 0$$

$$\theta = \theta_R = \text{constant}; \quad \phi = \phi_R = \text{constant}. \quad (\text{A.7})$$

*Bianchi type V*

$$\theta' = -\sin \theta, \quad \phi' = 0$$

$$\tan \left( \frac{\theta}{2} \right) = \tan \left( \frac{\theta_R}{2} \right) \exp [ - (\tau - \tau_R) ]$$

$$\phi = \phi_R = \text{constant}. \quad (\text{A.8})$$

*Bianchi type VII<sub>o</sub>*

$$\theta' = 0, \quad \phi' = -\cos \theta$$

$$\theta = \theta_R = \text{constant}$$

$$\phi = \phi_R - (\tau - \tau_R) \cos \theta_R. \quad (\text{A.9})$$

*Bianchi type VII<sub>h</sub>*

$$\theta' = -\sqrt{h} \sin \theta, \quad \phi' = -\cos \theta$$

$$\tan \left( \frac{\theta}{2} \right) = \tan \left( \frac{\theta_R}{2} \right) \exp [ - (\tau - \tau_R) \sqrt{h} ]$$

$$\phi = \phi_R + (\tau - \tau_R) - \frac{1}{\sqrt{h}} \ln \left\{ \sin^2 \left( \frac{\theta_R}{2} \right) + \cos^2 \left( \frac{\theta_R}{2} \right) \exp [ 2 (\tau - \tau_R) \sqrt{h} ] \right\}. \quad (\text{A.10})$$

*Bianchi type IX*

$$\theta' = 0, \quad \phi' = 0$$

$$\theta = \theta_R = \text{constant}$$

$$\phi = \phi_R = \text{constant.} \tag{A.11}$$

Hotspot focusing can be seen in the  $\theta$  propagation solutions in types V and VII<sub>h</sub>.

## Appendix B

*Bianchi type IX:*

The vorticity components are  $\omega^A = 1/4 e^{-3\alpha} \epsilon_{ABC} \epsilon_{DBC} u_D$  and hence the individual components in the  $E_A^\mu$  basis are

$$(\varpi^1, \varpi^2, \varpi^3) = 1/2 e^{-3\alpha} (\tilde{u}_1, \tilde{u}_2, \tilde{u}_3)$$

and hence the vorticity scalar is

$$\omega = 1/2 e^{-2\alpha} [(\tilde{u}_1)^2 + (\tilde{u}_2)^2 + (\tilde{u}_3)^2]^{1/2} \tag{B.1}$$

$$= 1/2 e^{-\alpha} [(u_1)^2 + (u_2)^2 + (u_3)^2]^{1/2}. \tag{B.2}$$

The  $T_{0i}$  Einstein equations give the constraints

$$\sigma_{BA} C_{Bi}^A - \sigma_{iC} C_{AC}^A = -8\pi G \rho_0 \exp(3\alpha_0 - 2\alpha) u_i. \tag{B.3}$$

If we expand this to second order (the left-hand sides vanish to linear order about isotropy in type IX, where  $C_{BC}^A \equiv \epsilon_{ABC}$ , then we have

$$1/2 \epsilon_{ijk} e^{-\alpha} (e^{2\beta} \sigma - \sigma e^{2\beta})_{jk} = 8\pi G \rho u_0 u_i. \tag{B.4}$$

For small anisotropies  $u_0 \sim -1$ ,  $\sigma_{ij} \sim \dot{\beta}_{ij}$  and

$$(e^{2\beta})_{ij} \approx \delta_{ij} + 2\beta_{ij},$$

so

$$\epsilon_{ijk} (\sigma\beta - \beta\sigma)_{jk} = 8\pi G e^\alpha \rho u_i. \tag{B.5}$$

Collins & Hawking give the approximate form for  $\beta_{ij}$  of

$$\beta_{ij} \approx F_{ij} \left( 1 - \frac{16}{5} \exp(\alpha - \alpha_m) \right) + G_{ij} \exp[-3/2(\alpha - \alpha_m)] \tag{B.6}$$

where  $F_{ij}$  and  $G_{ij}$  are constant matrices. This is a truncated series and will only be valid if  $\exp(\alpha - \alpha_m)$  is small compared with unity; thus, it is valid only far from the expansion maximum, that is, when

$$\exp(\alpha_0 - \alpha_m) = \frac{\Omega_0 - 1}{\Omega_0} \ll 1 \tag{B.7}$$

so we can consider only models with  $\Omega_0$  very close to unity. Using  $\sigma_{ij} = \dot{\beta}_{ij}$ , we split the shear into growing and decaying components,  $\sigma_{ij}^{(G)}$  and  $\sigma_{ij}^{(D)}$ , so we have

$$\sigma_{ij} = -\frac{16}{5} F_{ij} \dot{\alpha} \exp(\alpha - \alpha_m) - \frac{3}{2} G_{ij} \dot{\alpha} \exp[-3(\alpha - \alpha_m)/2] \tag{B.8}$$

and we decompose so that the constants  $F_{ij}$  and  $G_{ij}$  are given in terms of the present shear to Hubble ratio,

$$F_{ij} = -\frac{5}{16} \frac{\Omega_0}{(\Omega_0 - 1)} \left( \frac{\sigma_{ij}^{(G)}}{H} \right)_0 \quad (\text{B.9})$$

$$G_{ij} = -\frac{2}{3} \left( \frac{\Omega_0 - 1}{\Omega_0} \right)^{3/2} \left( \frac{\sigma_{ij}^{(D)}}{H} \right)_0. \quad (\text{B.10})$$

Equation (B.4) gives

$$\begin{aligned} & \frac{5}{24} \epsilon_{ABi} \left\{ \sigma_{j[B}^{(G)} \sigma_{A]j}^{(D)} \right\}_0 \left( \frac{\Omega_0 - 1}{\Omega_0} \right)^{1/2} \left\{ \frac{\dot{\alpha}}{H_0} \right\} \{ 3 \exp[-3(\alpha - \alpha_m)/2] - 16 \exp[-(\alpha - \alpha_m)/2] \} \\ & = 8\pi G \rho \exp(\alpha) u_i. \end{aligned} \quad (\text{B.11})$$

Using  $\rho = \rho_0 \exp[3(\alpha_0 - \alpha)]$  and  $8\pi G \rho_0 = 3H_0^2 \Omega_0$  for the Friedmann background, we have expressions for the velocity components

$$\begin{aligned} u_i &= \frac{5}{72} \epsilon_{ABi} \left\{ \frac{\sigma_{j[B}^{(G)} \sigma_{A]j}^{(D)}}{H} \right\}_0 \frac{(\Omega_0 - 1)^2}{\Omega_0^{3/2}} e^{\alpha_m} \\ & \times \llbracket 3 \exp[-(\alpha - \alpha_m)] - 16 \rrbracket [1 - \exp(\alpha - \alpha_m)] \end{aligned} \quad (\text{B.12})$$

so the *present* velocities are given by

$$(u_i)_0 = \frac{5}{72} \epsilon_{ABi} \left\{ \frac{\sigma_{j[B}^{(G)} \sigma_{A]j}^{(D)}}{H_0^2} \right\}_0 \frac{(16 - 13\Omega_0)}{\Omega_0(\Omega_0 - 1)^{1/2}} \quad (\text{B.13})$$

and the velocities at the emission redshift,  $z_E$ , of last scattering are

$$(u_i)_E = \frac{5}{72} \epsilon_{ABi} \left\{ \frac{\sigma_{j[B}^{(G)} \sigma_{A]j}^{(D)}}{H_0^2} \right\}_0 \left( \frac{1 + \Omega_0 z_E}{1 + z_E} \right)^{1/2} \frac{(16 - 13\Omega_0 + 3\Omega_0 z)}{\Omega_0(\Omega_0 - 1)^{1/2}}. \quad (\text{B.14})$$

The solution of the geodesic equations for type IX given in Appendix A shows that we have constant  $\theta = \theta_0$  and  $\phi = \phi_0$ , so there is neither the geodesic focusing nor the spiralling effects found in the type V and VII universe models.